Multiband Antenna Design Based on Descartes Circle Theorem

Majda. I. Abdraba Mohammed

Submitted to the
Institute of Graduate Studies and Research
in partial fulfilment of the requirements for the degree of

Master of Science
in
Electrical and Electronic Engineering

Eastern Mediterranean University
July 2018
Gazimağusa, North Cyprus

Approval of the Institute of Graduate Studies and Research

Assoc. Prof. Dr. Ali Hakan Ulusoy
Acting Director

I certify that this thesis satisfies all the requirements as a thesis for the degree of Master of Science in Electrical and Electronic Engineering.

Prof. Dr. Hasan Demirel
Chair, Department of Electrical and Electronic Engineering

We certify that we have read this thesis and that in our opinion it is fully adequate in scope and quality as a thesis for the degree of Master of Science in Electrical and Electronic Engineering.

Asst. Prof. Dr. Rasime Uyguroğlu
Supervisor

Examining Committee

1. Prof. Dr. Hasan Demirel _____

2. Assoc. Prof. Dr. Mehmet Kuşaf _____

3. Asst. Prof. Dr. Rasime Uyguroğlu _____

ABSTRACT

Self-similar slots, known as fractal geometries, are widely used to enhance the bandwidths of the patch antennas. In this study, Descartes Circle Theorem (DCT) is used to obtain the fractal geometries for four iterations. Dual and wideband are achieved by applying CPW-fed Circular Fractal Antenna (CFA) for half- wave length applications.

The design and simulation of this study are carried out by using CST Microwave Simulation Software. Two wideband responses were obtained, 23 % at resonance 1.08 GHz, and 3 % at 1.82 GHz. The resonant frequency was lowered by 51.3 %. The directivity was 6.54 dB when the original design was deployed where it was 3.97 dB and 6.72 dB for the resonant frequencies 1.08 GHz and 1.82 GHz respectively. Additionally, U and H ground cut designs are proposed and simulated. Bandwidths of 45 % at resonate frequency of 1.004 GHz and 55.9 % at resonate frequency of 0.958 GHz were achieved respectively.

Keywords: circular fractal antenna, CPW-fed, Descartes Circle Theorem, self –similar iteration, bandwidth

ÖZ

Fraktal geometriler olarak bilinen kendinden benzer geometrik yapılar, yama antenlerinin bant genişliklerini geliştirmek için yaygın olarak kullanlmaktadır. Bu çalışmada, Descartes daire teoremi, fraktal geometrileri elde etmek için kullanılmıştır. Yarım dalgaboyu uygulamaları için, uygulanan CPW beslemeli dairesel fraktal antenler ile, çift ve geniş bant elde edilmiştir.

Bu çalışmanın tasarımı ve simülasyonu CST Mikrodalga Simülasyon Yazılımı kullanılarak gerçekleştirilmiştir. Rezonant frekansı 1.08 GHz'de ve 1.82 GHz'de sırası ile % 23 ve % 3 iki geniş bant elde edilmiştir. Rezonans frekansı % 51.3 oranında düşürülmüştür. Özgün tasarım yöntemi uygulandığında 6.54dBi olan yönelimin, dördüncü derece iterasyon uygulaması için, 1.08 ile GHz 1.82 GHz resonat frekanslarında sırasıyla 3.97 dB ve 6.72 dB değerlerine yükseldiği görülmüştür.

Ayrıca, zemin üzerinde uygulanan U ve H şeklindeki yarıklar vasıtası ile, sırasıyla 1.004 GHz'te % 45 ve 0.958 GHz'te de % 55.9 bant genişliği elde edilmiştir.

Anahtar Kelimeler: dairesel fraktal slot anteni, CPW beslemeli, Descartes daire teoremi, kendinden farklı iterasyon, bant genişliği

ACKNOWLEDGEMENT

All praise is due to Allah Subhanahu Wataala for his blessing and guidance. In my journey in my academic pursuit, there are many people to who I am thankful for their generosity. First, I am sincerely grateful to my advisor **Asst. Prof. Dr. Rasime Uyguroğlu** for the continuous support throughout my study for master's degree and eventually, my thesis, which is a fundamental requirement for the final award. I must not forget to mention her patience, motivation, and immense knowledge I have benefited during researching and writing my thesis. I could not have imagined having a better advisor and mentor as you.

Many special thanks to my family. Words are not sufficient to express how grateful I am to my mother and father for the numerous sacrifices you have made for my welfare. I also thank my sisters and my brother who encouraged me and prayed for me throughout the time of my research. I acknowledge the efforts of my mother-in law, father-in-law, and my friend Lara Mohammed. I have tremendous gratitude to my beloved husband, Moataz Saied for believing in me and supporting me in everything I do.

I cannot thank you all enough for the various roles you have played in encouraging me throughout this memorable stage in my life.

TABLE OF CONTENTS

LIST OF TABLES

LIST OF FIGURES

LIST OF SYMBOLS AND ABBREVIATIONS

BW	Bandwidth
CFA	Circular Fractal Antenna
CPW	Coplanar Waveguide
CST	Computer Simulation Technology
D	Diameter of aperture
DCT	Descartes Circle Theorem
f_o	The operation frequency
f_1	Lower frequency
f_2	Upper frequency
F	Fractal scaling factor
FEA	Finite Element Analysis
FR4	Flame Retardant 4
GSM	Global System for Mobile communications
h	The thickness of FR4 substrate
R	Radius of the patch
RF	Radio Frequency
t	The thickness of the patch and the ground plane
UWB	Ultra Wide Bandwidth
W1	The width of substrate and ground plane
W2	The length of substrate and ground plane
WLAN	Wireless Local Area Network
w	The width of feed line
ε_r	Relative permittivity

Chapter 1

INTRODUCTION

1.1 Thesis Overview

Coplanar waveguide (CPW) antennas constructed dielectric insulating materials, provide wider bandwidth compared to the conventional microstrip patch antennas. In wireless communication, the wide band antennas have received increasing interests and CPW became more popular compared to the typical microstrip antennas [1]. Beside the wideband advantage, they have good impedance matching capabilities and the radiation loss is less. Because of these properties of CPW's, they can be used as broadband and dual-band antennas. However, there is always need for trial and error mode to get the necessary configurations for designing and realizing the desired applications. The bandwidth of CPW-fed can be extend by using a metallic strip in the antenna aperture [2].

The innovative configuration of the circular shaped opening is depicted with an appropriate internal connector, which can be applied to broadband response and high gain antennas. Applying the fractal antenna is also one of the methods that can be used to provide multi-frequency operation band. Thus, fractals are quantified curved forms, which are similar to the self, replicating themselves in different scales [3].

The use of fractal geometry in the patch antenna increases the effective length, or increases the outside environment and can receive or transmit electromagnetic

radiation [4]. The main properties of the fractal antennas are self-similarity and space-filling characteristics of the design [5]. Generally speaking, fractal geometry is one of the most popular methods that can be used to get ultra wide bandwidth (UWB). In this study, the design of circular fractal slot antenna is presented and synthesized by using DCT.

1.2 Thesis Objective

The objective of this thesis is to obtain wider bandwidth for the circular patch antenna.

1.3 Thesis Contribution

The CPW-fed and circular fractal technique have been applied, wideband and dual-band designs were achieved.

1.4 Thesis Organization

The first chapter illustrates the effect for CPW-fed structure on fractals in antenna design. Chapter 2 includes the definition of antenna, parameters of antenna and ways to feed it. Chapter 3 demonstrates the history, definition and the most popular types of fractal antennas, while Chapter 4 illustrates the design methodology and presents the simulation results of the CFA where Chapter 5 illustrates the results of the ground cut design. Chapter 6 presents the conclusion and possible areas of future research.

Chapter 2

PLANAR ANTENNAS

2.1 Definition of Antennas

Antennas are very important components of communication systems [6]. The antennas are devices which are able to transmit and receive signals. Antennas are reciprocal which means that they have same characteristics in the transmitting and receiving modes. The main definition of antennas is resonant devices operating efficiently over a relatively narrow frequency band. A graphical representation of the radiated power in space is called a radiation pattern. This pattern may be distributed in a certain direction in free space.

2.2 Patch Antenna

2.2.1 Patch Antenna Definition

The microstrip patch antenna [6] consists of substrate between the ground and the patch. Patch antenna can be classified as single-element resonant antenna. Figure 2.1 shows the different types of patch antennas, and the most famous types of patch antennas used are the rectangular and circular patches.

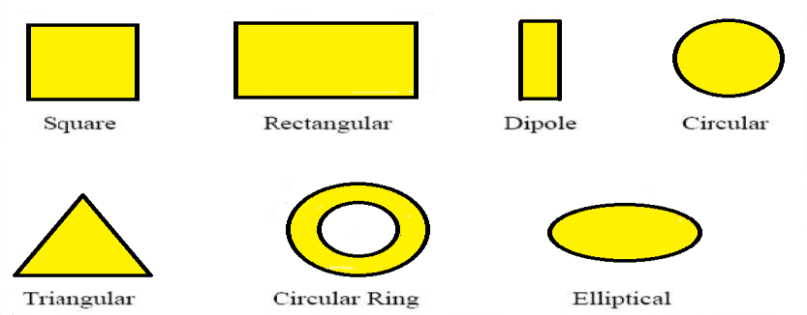

Figure 2.1: Types of Patches [6]

2.2.2 Patch Antenna Properties:

Some important properties of these kind of antennas are as follows:

Advantages of patch antennas are:

- Small size.
- Low profile.
- Lightweight.
- Conformable to planar and non-planar surfaces.
- Simple and cheap to manufacture.

Disadvantages of patch antenna are:

- Low efficiency.
- Narrow bandwidth.
- Low RF power.

2.2.3 Feeding Techniques

There are many methods of feed techniques available but some of the common techniques are [7][8]:

- Microstrip line.
- Coaxial probe.
- Proximity coupling.
- Aperture coupling.
- Co-planner waves guide feed.

In this study a coplanar waveguide (CPW) feed is used.

2.2.3.1 CPW Feeding

Coplanar Waveguides (CPWs) are transmission lines consisting of a centre conductor strip and two ground conductor planes. All three conductors are placed on the same side of a dielectric substrate, as shown in Figure 2.3.

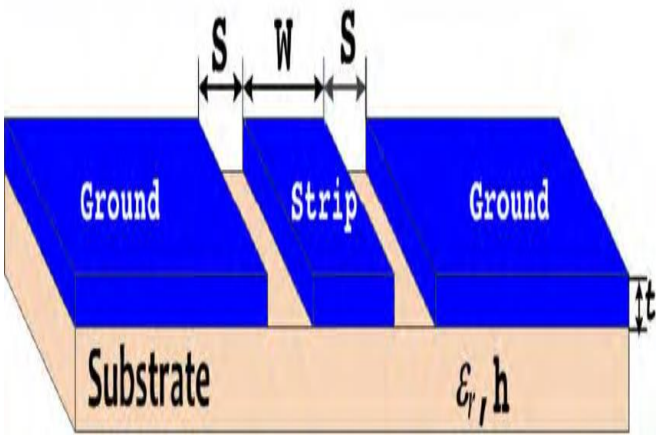

Figure 2.2: CPW- Fed [10]

Coplanar waveguide structure, has wider bandwidth, better impedance matching, lower radiation loss and easy connection [9].

Chapter 3

LITERATURE SURVEY OF FRACTAL ANTENNA

3.1 History of Fractal

In the 17th century, Gottfried Leibnitz was the first person who developed the fractal structures when he wrote about recursive self-similarity [11]. It was not until after two centuries that the first published fractal emerged with Karl Weierstrass' publication of the first fractal graph in the year 1872. In contemporary practice, mathematicians are still unable to describe and analyse the fractal structure because of the unavailability of the necessary tools to do so, as a result, they have referred to fractals simply as "mathematical monsters".

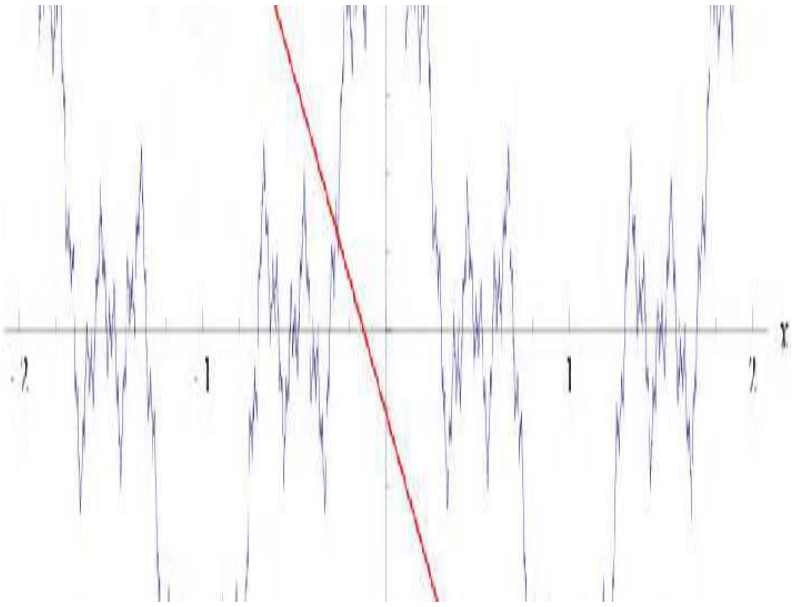

Figure 3.1: First Graph for Fractal [11]

There are other notable attempts in the development of fractal. For instance, George Cantor in 1883 published a subset of interval [0;1], what is known today as Cantor set. The cantor set is an iteration of set rules, which later inspired a great breakthrough by Helge Von Koch who in 1904 designed many of the new fractals with geometric repeaters including the most famous fractal Koch snowflake. One decade later, WaclawSierpinski constructed more fractals including the Sierpinski triangle. In 1918 Pierre Fatou and Gaston Julia designed new fractals with different functions on the complex plane. At the same time Felix Hausdroff notably defined that the dimension of fractal does not need to be an integer.

In 1950, the first fractal antennas invented by Isbell and Du Hamel were fractal arrays. Though the fractal arrangement of antennas were not initially identified to have contained self-similarities because their properties were used in TV antenna. In 1995 Cohen published the first fractal antenna design.

3.2 Definition of Fractal Antenna

In the application of modern wireless communication systems, wider bandwidth, multiband and low profile antennas are in high demand. One of the ways of achieving these properties is to use fractal shaped antenna elements. Traditionally, each antenna operates with either single or dual frequency bands, where different antennas are needed for different applications.

For fractal antenna designs, a self-replicating fractional designs are used to maximize the effective length of materials that can receive or transmit electromagnetic radiation within a given surface area or volume.

3.3 Types of Fractal Antenna

Due to the wideband properties of the fractal antennas, antenna engineers used different types of fractals in the designs. Today, the most commonly used fractals are Koch curve [12], Sierpinski gasket [13], Sierpinski carpet, and the cantor set geometry [14]. In this design circular fractal antenna is used to present alternative broadband antennas [15].

3.4 Properties of Fractal Antenna

3.4.1 Advantages of Fractal Antenna [14]:

1-Smaller size with good performance.

2- Multiband/ wideband.

3- Better input impedance matching.

4- Frequency independent.

5- Lower cost.

6- Polarization and phasing of FEA also possible.

3.4.2 Disadvantages of Fractal Antenna:

1- Lower gain.

2- Complex geometry.

3- The benefits begin to diminish after first few iterations.

Chapter 4

ANTENNA DESIGN AND METHODOLOGY

4.1 Antenna Design

Fractals having circular apertures are considered in this study, because of their easy design capabilities to the iterative methods. In this study, DCT is used to obtain the radii of every circle of designs [16] [17].

According to DCT, if four circles are touching to each other in a plane, with disjoint interiors, their surfaces satisfy equation 4.1.

$$(a_{i+} b_{i+} c_{i+} d_i)^2 = 2(a_i^2 + b_i^2 + c_i^2 + d_i^2),\ i = 1, 2\ldots \quad (4.1)$$

Where $a_i = 1/r_{ai}$, $b_i = 1/r_{bi}$, $c_i = 1/r_{ci}$ and $d_i = 1/r_{di}$, and r_{ai}, $r_{bi,}$ $r_{ci,}$ r_{di} are the radii of the circles.

Bends are defined by unit vectors, and signs of the unit vectors are obtained from their direction. For normal internal routing, the radius is given by r, indicating normal to the outside and –r indicates the unit vector inside. Once the first phase of the four circle equation can be applied, the next step is to determine the smallest circle size for any of the three original circles. Using a stage-to-stage step processes, i = 1, 2, …, and this is designated as the self-similar iteration design.

4.2 Initial Fractal Configuration

The curvature with a normal pointing outward r= -1, provided that the original circular aperture denotes a unit circle. From the self-similar design of the iteration at i=1, the radii of each of the three identical inner circles [18], as shown in figure 4.1 (a) are calculated by equation 4.2 and expressed as $r_{b1} = r_{c1} = r_{d1} = 3/ (3+2\sqrt{3})$. So the curvatures about the initial four circles as given by equation 4.2.

$$(-1, \frac{3+2\sqrt{3}}{3}, \frac{3+2\sqrt{3}}{3}, \frac{3+2\sqrt{3}}{3}) \tag{4.2}$$

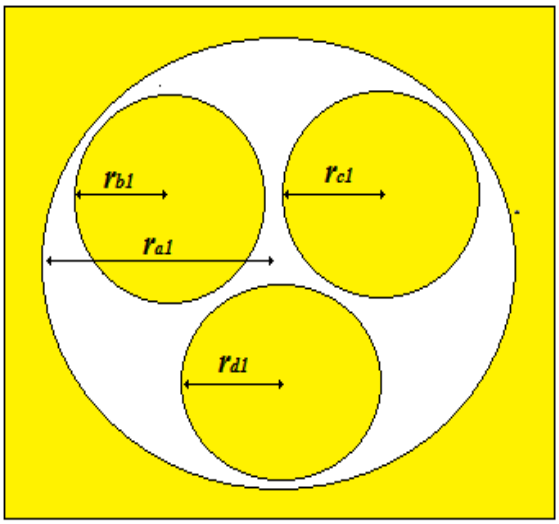

(a)

Figure 4.1 (a): First Stage

At the second stage, the radii of five circles are obtained from the initial four circles in the first stage.

$$e^{I}_{2-1} = a_2 + b_2 + c_2 + 2\sqrt{a_2b_2 + a_2c_2 + b_2c_2} \tag{4.3}$$

$$e^{II}_{2-1} = a_2 + b_2 + d_2 + 2\sqrt{a_2b_2 + a_2d_2 + b_2d_2} \tag{4.4}$$

$$e^{III}_{2-1} = a_2 + c_2 + d_2 + 2\sqrt{a_2c_2 + a_2d_2 + c_2d_2} \quad (4.5)$$

$$e^{I}_{2-2} = b_2 + c_2 + d_2 + 2\sqrt{b_2c_2 + b_2d_2 + c_2d_2} \quad (4.6)$$

Where $e^{I}_{2-1} = e^{II}_{2-1} = e^{III}_{2-1} = 1/r_{e2-1}$, $e^{I}_{2-2} = 1/r_{e2-2}$ and r_{e2-1} and r_{e2-2} are the radii of the circles. As a result, the radii are $re_{2-1} = 1/(1+2\sqrt{3})$ and $re_{2-2} = 1/(7+4\sqrt{3})$ as illustrated in figure 4.1 (b).

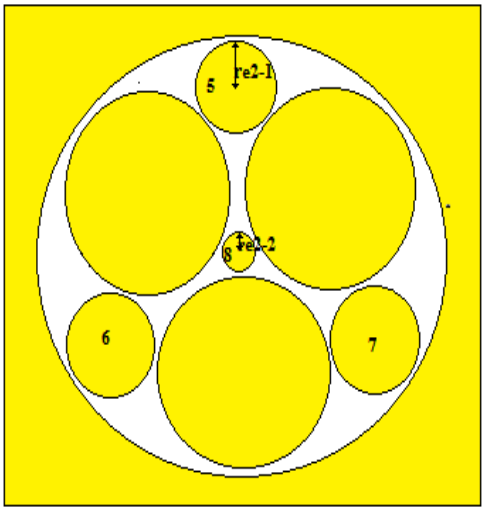

(b)

Figure 4.1 (b): Second Stage

In a similar way, in the third stage, a set of two circles is selected from the initial four circles obtained in the first stage and the radii of five circles were obtained in the second stage to determine the radii of nine circles. The radii of twelve circles obtained are summarized by equations 4.7-4.18.

$$(-1, \frac{3+2\sqrt{3}}{3}, \frac{3+14\sqrt{3}}{3}, 1+2\sqrt{3}) \quad (4.7)$$

$$(-1, \frac{3+14\sqrt{3}}{3}, \frac{3+2\sqrt{3}}{3}, 1+2\sqrt{3}) \quad (4.8)$$

$$(-1, \frac{3+2\sqrt{3}}{3}, 1+2\sqrt{3}, \frac{3+14\sqrt{3}}{3}) \quad (4.9)$$

$$(-1, \frac{3+14\sqrt{3}}{3}, 1+2\sqrt{3}, \frac{3+2\sqrt{3}}{3}) \quad (4.10)$$

$$(-1, 1+2\sqrt{3}, \frac{3+2\sqrt{3}}{3}, \frac{3+14\sqrt{3}}{3}) \quad (4.11)$$

$$(-1, 1+2\sqrt{3}, \frac{3+14\sqrt{3}}{3}, \frac{3+2\sqrt{3}}{3}) \quad (4.12)$$

$$(7+4\sqrt{3}, 17+10\sqrt{3}, \frac{3+2\sqrt{3}}{3}, \frac{3+2\sqrt{3}}{3}) \quad (4.13)$$

$$(7+4\sqrt{3}, \frac{3+2\sqrt{3}}{3}, 17+10\sqrt{3}, \frac{3+2\sqrt{3}}{3}) \quad (4.14)$$

$$(7+4\sqrt{3}, \frac{3+2\sqrt{3}}{3}, \frac{3+2\sqrt{3}}{3}, 17+10\sqrt{3}) \quad (4.15)$$

$$(\frac{3+2\sqrt{3}}{3}, \frac{3+2\sqrt{3}}{3}, \frac{21+20\sqrt{3}}{3}, 1+2\sqrt{3}) \quad (4.16)$$

$$(\frac{3+2\sqrt{3}}{3}, \frac{21+20\sqrt{3}}{3}, \frac{3+2\sqrt{3}}{3}, 1+2\sqrt{3}) \quad (4.17)$$

$$(\frac{3+2\sqrt{3}}{3}, \frac{3+2\sqrt{3}}{3}, 1+2\sqrt{3}, \frac{21+20\sqrt{3}}{3}) \quad (4.18)$$

As illustrated in figure 4.1c, the radii of the twelve circles with r_{f3-1}=3/(3+14$\sqrt{3}$), r_{f3-2}= 1/(17+10$\sqrt{3}$), and r_{f3-3}= 3/(21+20$\sqrt{3}$) are obtained.

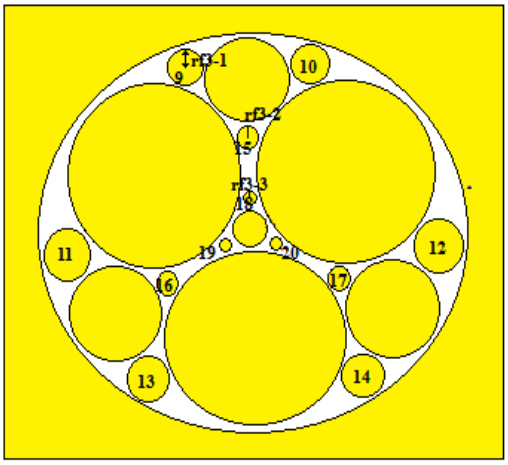

(c)

Figure 4.1 (c): Third Stage

Figures 4.1 (a, b and c) illustrate that: circles 2,3 and 4 are equal, and circles 5, 6 and 7 are equal, while circles 9, 10, 11, 12, 13 and 14 are equal. The same applies to circles 15, 16, 17 as well as 18, 19 and 20. So we conclude that Descartes Circle Theorem is dependent on circles (1) and (8).

$$d_i = a_i + b_i + c_i \pm 2\sqrt{a_i b_i + b_i c_i + c_i a_i} \tag{4.19}$$

The sign (+) is relevant to calculate the small circle denoted by number 8, and the sign (-) is for the biggest circle denoted by number 1.

4.3 Design Map

The strategy [19], is applied by the equations below to calculate the radii, as it is clear in figure 4.1 (d).

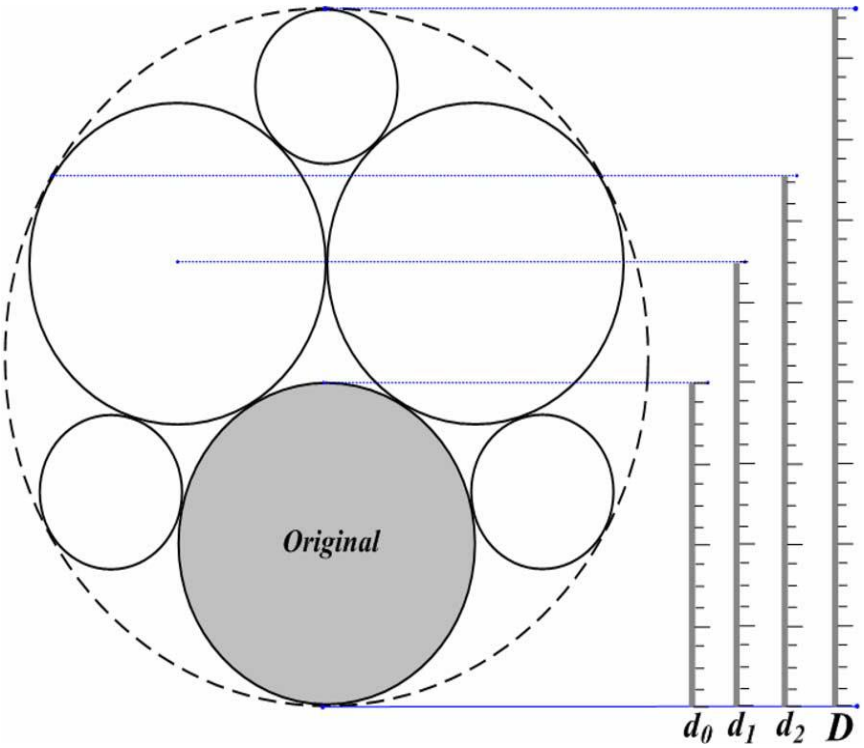

Figure 4.1 (d): Design Map [19]

$$d_0/d_1 = 2/ (1+\sqrt{3}) \quad (4.19)$$

From d_0 we can obtain D by the relation of equation 4.20.

$$D/d_0 = 1/ (3/3+2\sqrt{3}) \quad (4.20)$$

d_2 is calculated by the relation given in equation 4.21.

$$d_0:d_2 = 1: (3+2\sqrt{3}/4) \quad (4.21)$$

4.4 Antenna Results and Discussion

The dimensions of the CPW-fed circular fractal slot antenna are illustrated in table 4.1 below.

Table 4.1: Dimensions of Antenna

Dimensions of the antenna	Values	Definition of the dimensions
W1 (mm)	*120*	The substrate width
W2 (mm)	*120*	The substrate length
h (mm)	*1.6*	The thickness of FR4 substrate
ε_r	*4.4*	Relative permittivity
w (mm)	*3*	The width of feed line
D (mm)	*100*	Diameter of aperture
r_{d1} *(mm)*	*23.4*	The radius of inner conductor
f_o *(GHz)*	*2.22*	The operation frequency
t (mm)	*0.035*	The thickness of the patch and the ground plane

The actual radius can be calculated by using the equation specified below by equation 4.22.

$$R=\frac{F}{\sqrt{1+\frac{2h}{\pi\varepsilon_r F}\left[\ln\left(\frac{\pi F}{2h}\right)+1.7726\right.}} \quad (4.22)$$

Where;

$$F=\frac{8.791\times10^{9}}{f_r\sqrt{\varepsilon_r}} \quad (4.23)$$

Where R is the radius of the patch, ε_r is the relative permittivity, h is the substrate height, f_r is the resonant frequency and F is the fractal scaling factor. Figure 4.2 illustrates the first design that was simulated by using CST simulation software.

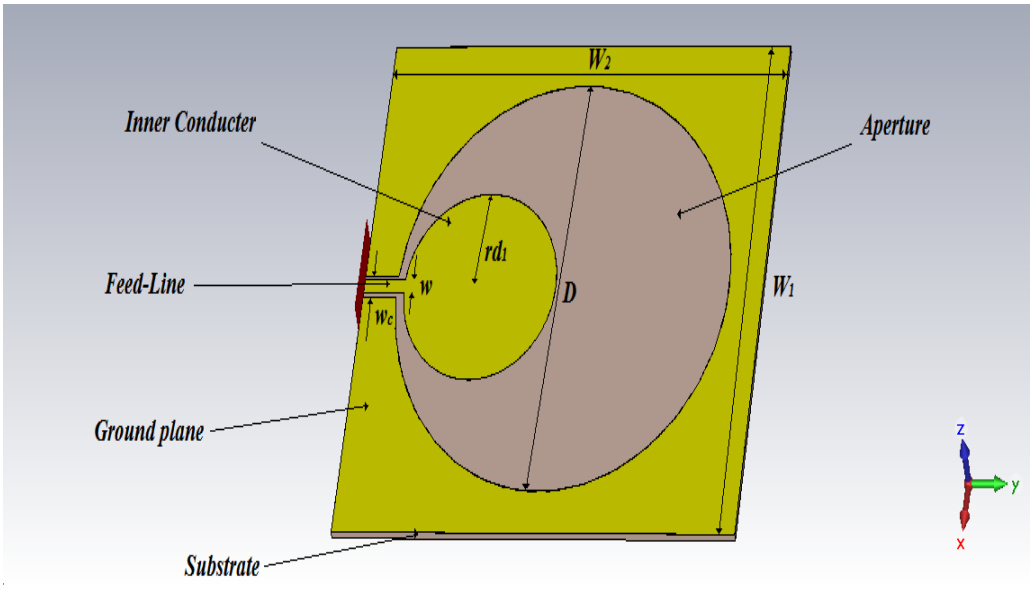

Figure 4.2: Original Design

Figure 4.3 (a) below describes S parameter in dB. As clearly can be seen the frequency of the antenna is resonant at 2.2249 GHz with return loss of -38.762 dB, and the bandwidth at -10 dB is 26.9 %. This is calculated in equation 4.24.

$$BW=\frac{f_2-f_1}{f_r} \quad (4.24)$$

Where f_r is the resonant frequency, f_2 is the maximum frequency and f_1 is the minimum frequency.

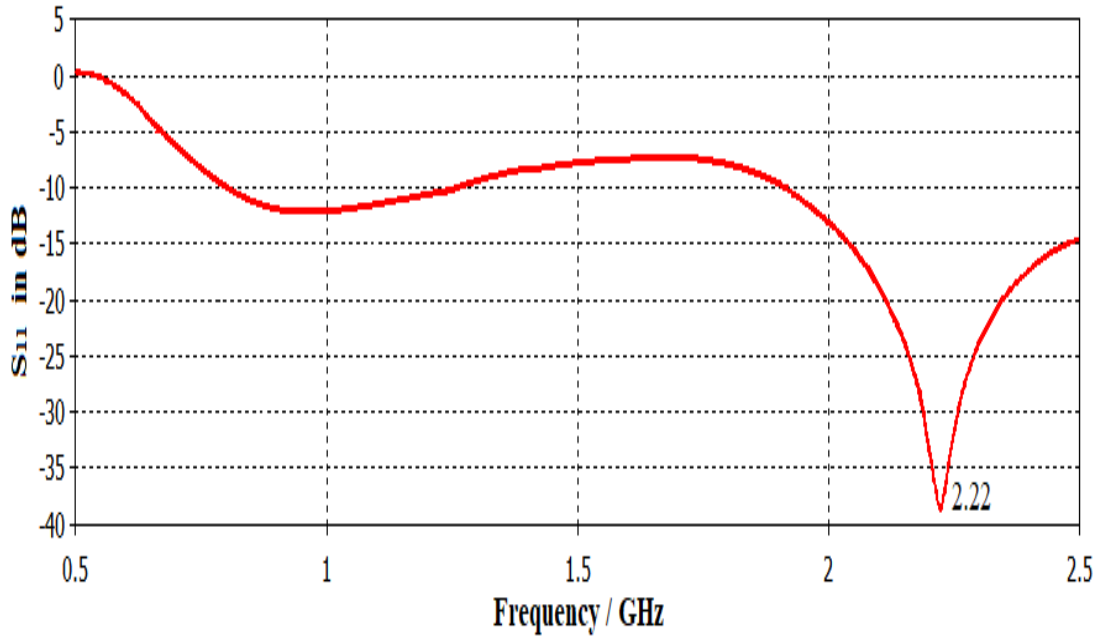

Figure 4.3 (a): Return Loss of Original Design

When compared with result of the reference paper, it can be noted that both are nearly like each other as clearly illustrated in figure 4.3 (b).

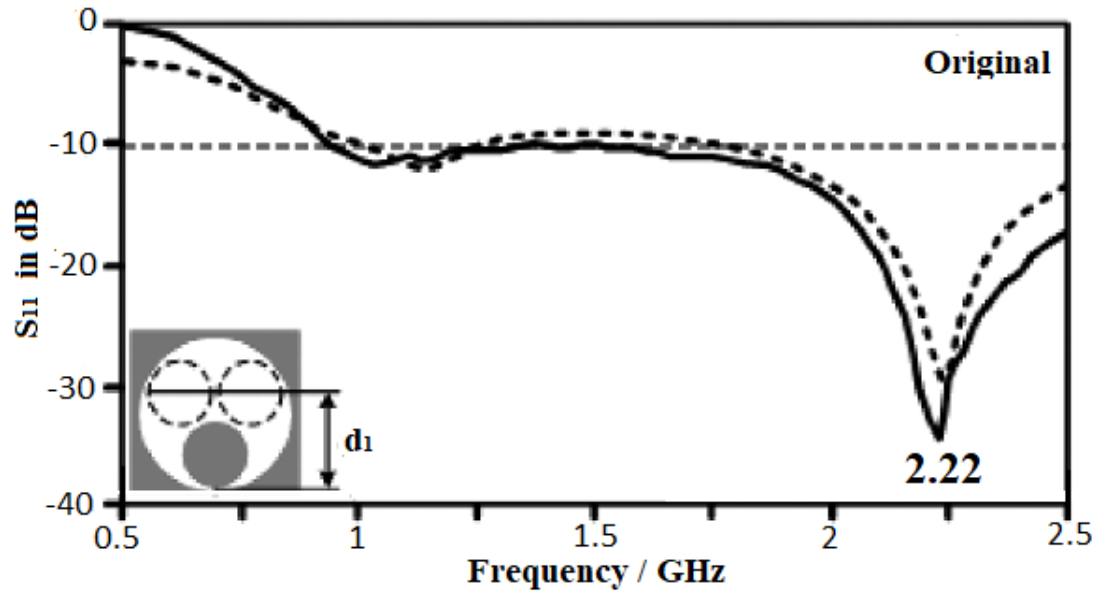

Figure 4.3 (b): S_{11} Curve of [19]

Radiation patterns for 3D and 2D plots of the original antenna in figures 4.4 (a) and 4.4 (b) clarifies that the gain and directivity at resonant frequency 2.22 GHz are 6.75 dB and 6.54 dB respectively.

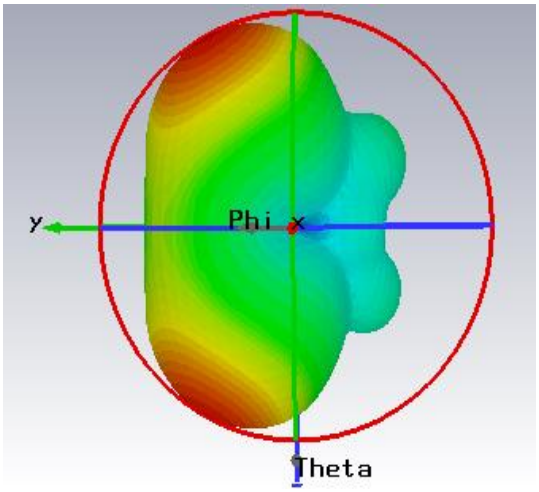

Figure 4.4 (a): 3D Plot of the Radiation Pattern of Original Design

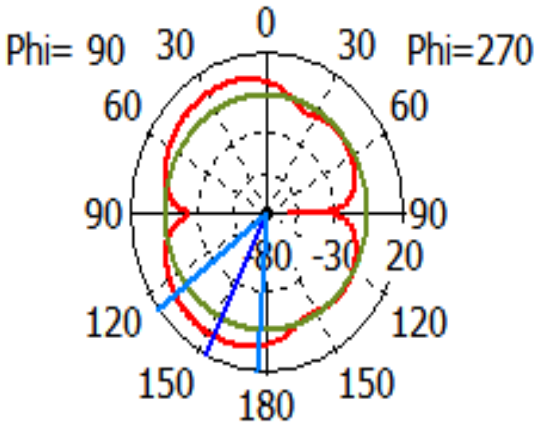

Figure 4.4 (b): Polar Plot of Radiation Pattern of Original Design

Stage 1 design is shown by Figure 4.5, where the Descartes Circle Theorem was applied, and figure 4.6 (a) illustrates the first result after using the fractal antenna. The indication is that it was a good result, where the return loss was -32 dB at first frequency 1.67 GHz and second frequency 1.926 GHz, the return loss was -37.862 dB. The bandwidth efficiency of all the two resonance frequencies is 31.7 %.

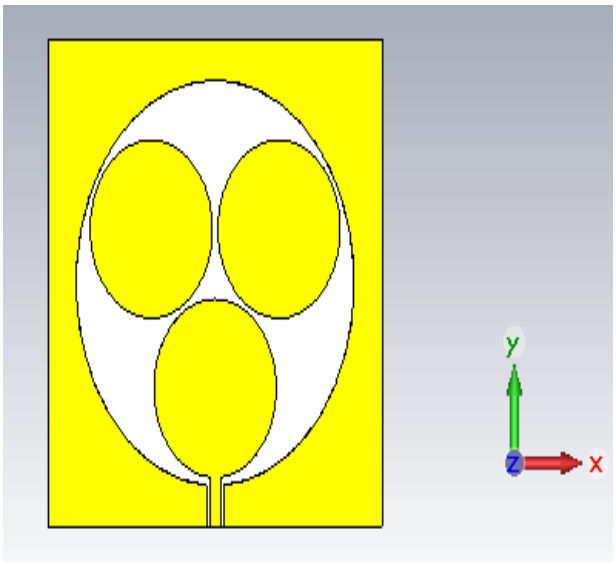

Figure 4.5: First Stage

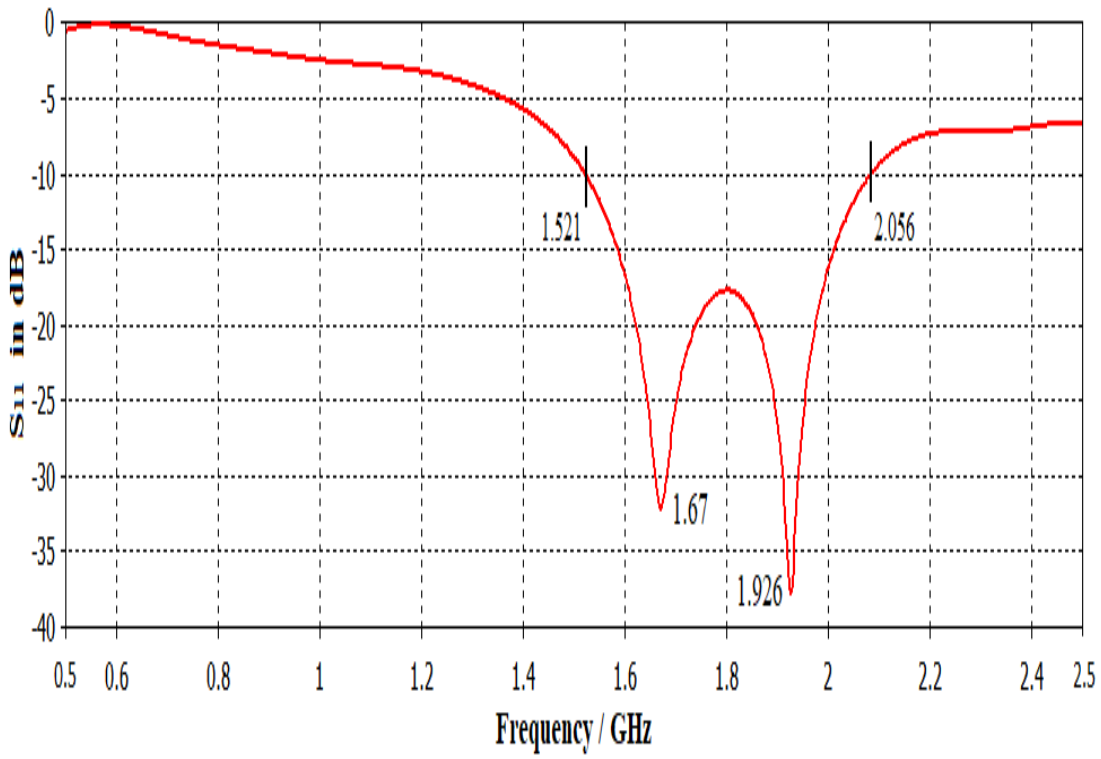

Figure 4.6 (a): Return Loss of First Stage

In current study, the return loss at first resonant frequency, appears to be similar to that which was derived from the design in the paper at 1.67 GHz.

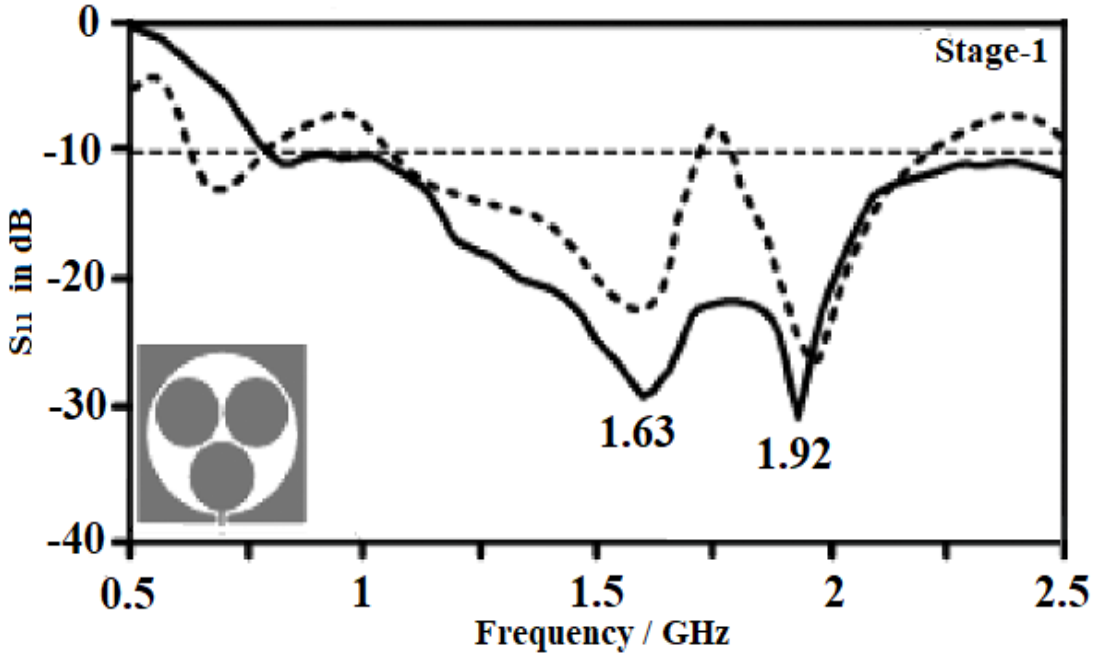

Figure 4.6(b): Return Loss of [19]

As clearly seen in the radiation pattern in figure 4.7 (a, b, c and d) the gain and directivity at first resonant frequency 1.67 GHz are 3.97 dB, 3.85 dB respectively, and 4.83 dB, 4.8 dB for the second frequency 1.926 GHz.

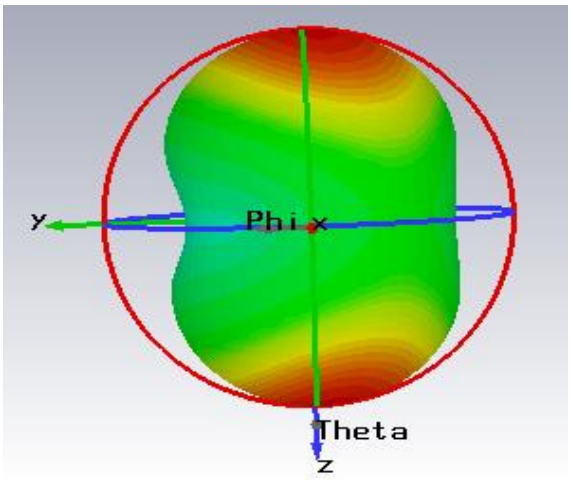

Figure 4.7 (a): 3D Radiation Pattern of First Stage at 1.67 GHz

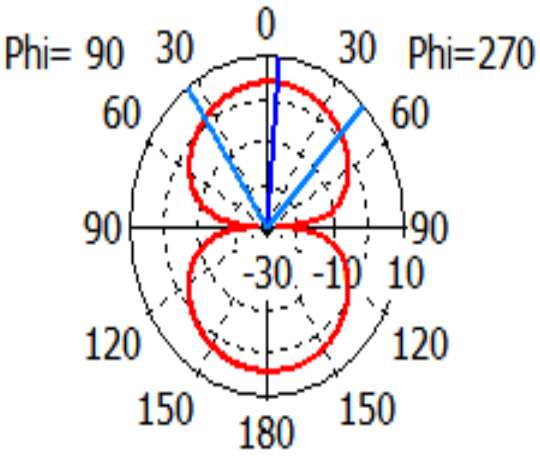

Figure 4.7 (b): Polar Radiation Pattern of First Stage at 1.67 GHz

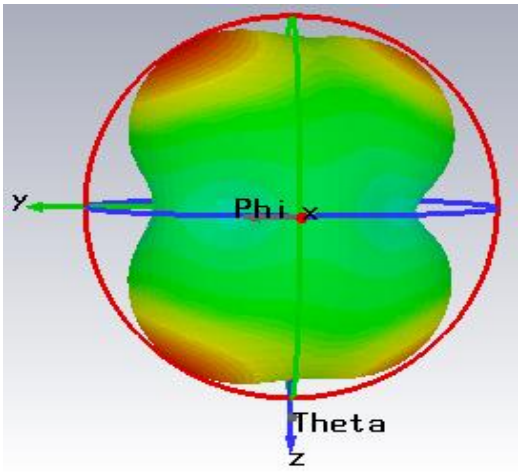

Figure 4.7 (c): 3D Radiation Pattern of First Stage at 1.926 GHz

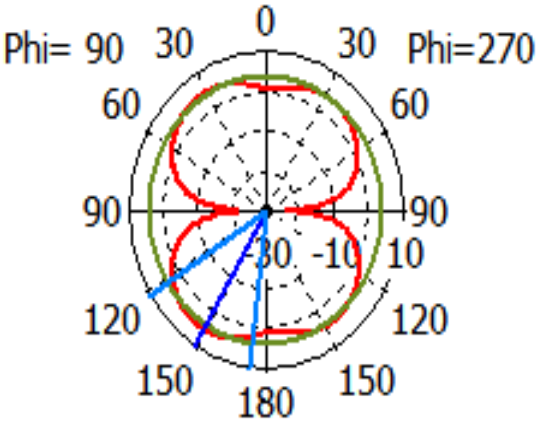

Figure 4.7 (d): Polar Radiation Pattern of First Stage at 1.926 GHz

Figure 4.8 shows the design of the second stage that consist of six circles. The return loss is given as -48.154 dB and bandwidth efficiency 33.1 % at first resonant frequency 1.16 GHz. Also as shown in figure 4.9 (a) at the other frequency 1.87 GHz the return loss was -21 dB and the bandwidth efficiency is 4 %.

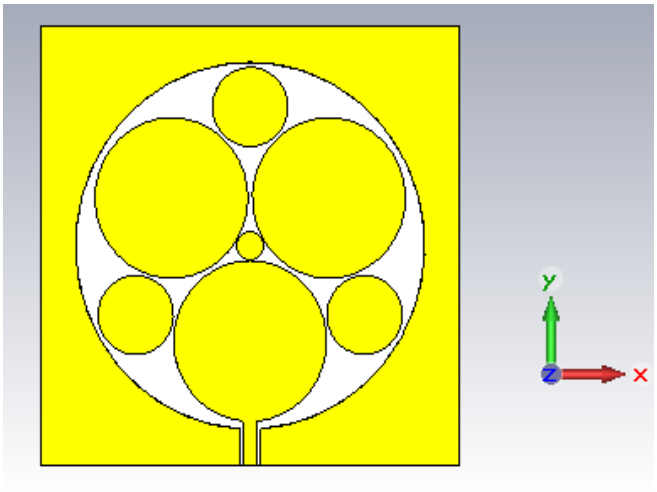

Figure 4.8: Second Stage

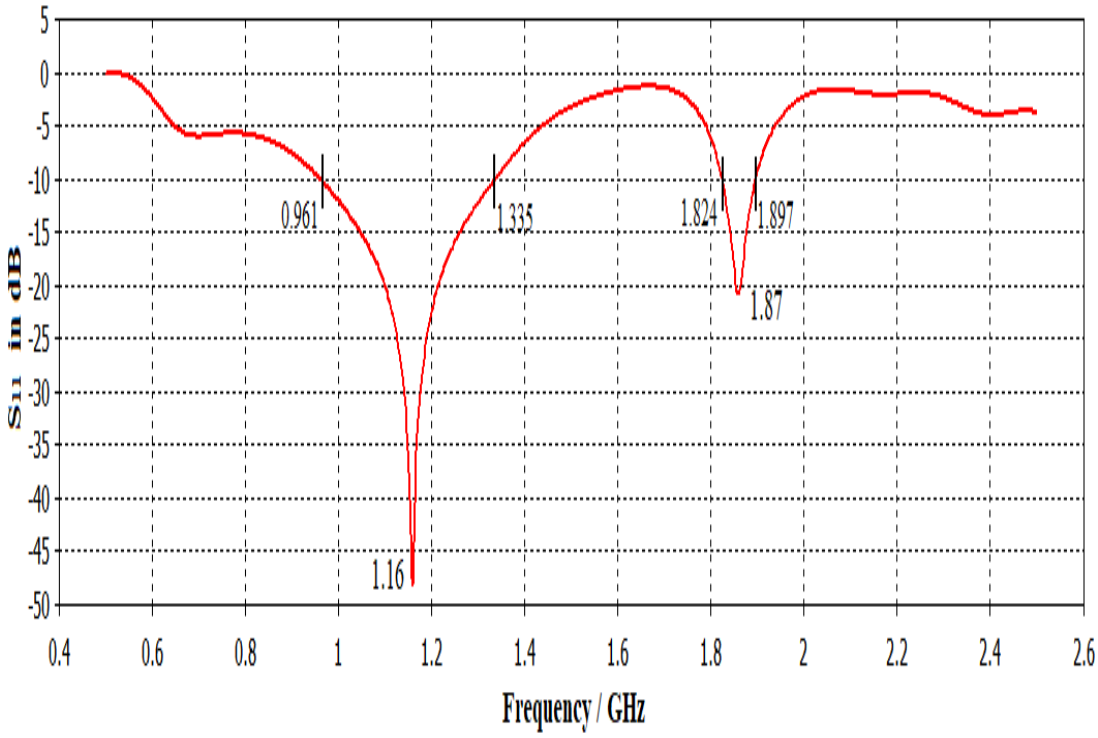

Figure 4.9 (a): Return Loss of Second Stage

Figure 4.9 (b) illustrates the return loss of paper, where there is a similarity at the second resonant frequency, but at first resonant frequency it had wideband at 1.13 GHz and in current study design, we obtained a wide bandwidth at 1.16 GHz.

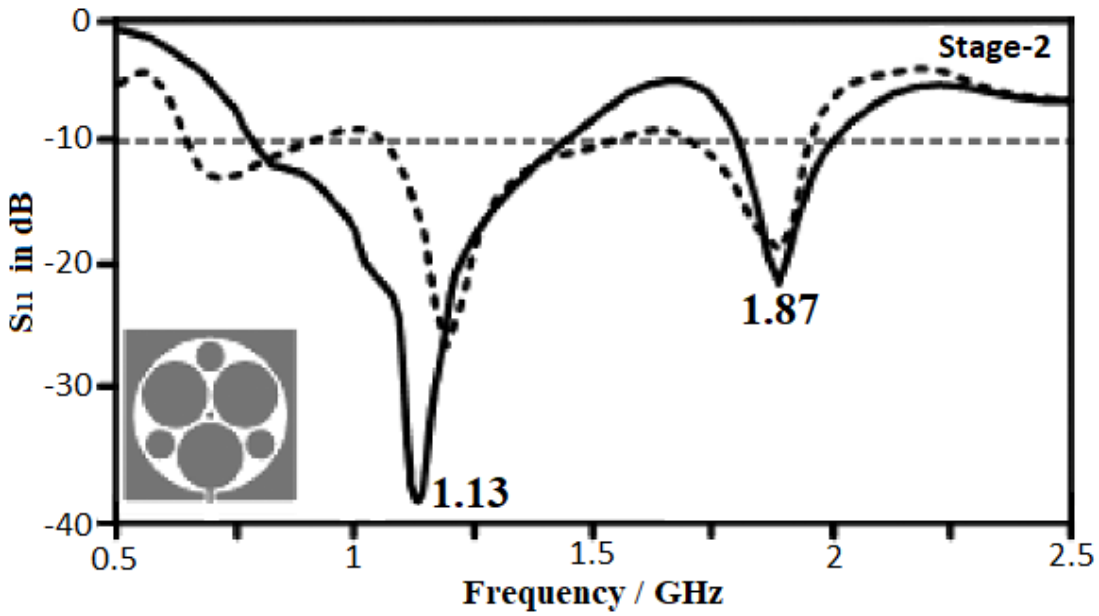

Figure 4.9 (b): Return Loss of [19]

On the other side, the shape of radiation pattern in figures 4.10 (a, b, c and d), illustrated the directivity and gain at 1.16 GHz are 4.14 dB and 4.41 dB respectively, and 6.65 dB, 6.55 dB at 1.87 GHz.

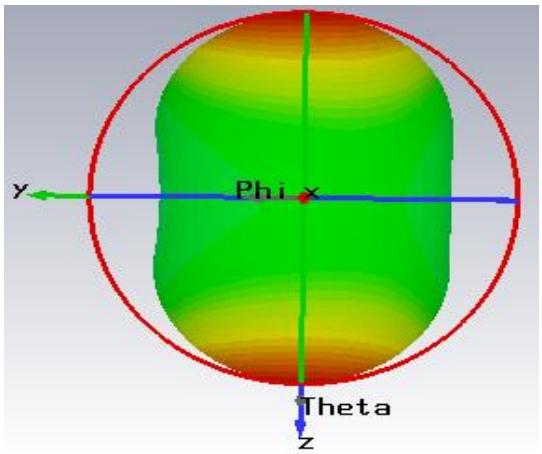

Figure 4.10 (a): 3D Radiation Pattern of Second Stage at 1.16 GHz

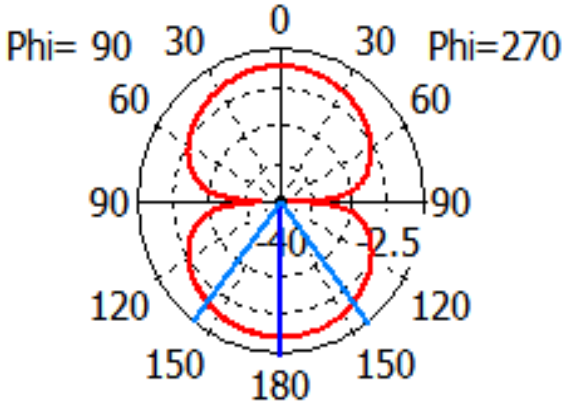

Figure 4.10 (b): Polar Radiation Pattern of Second Stage at 1.16 GHz

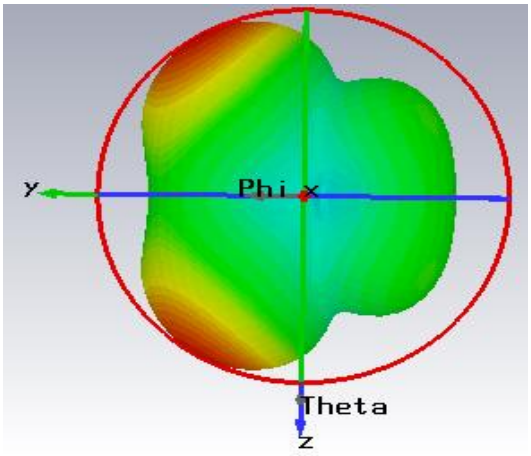

Figure 4.10 (c): 3D Radiation Pattern of Second Stage at 1.87 GHz

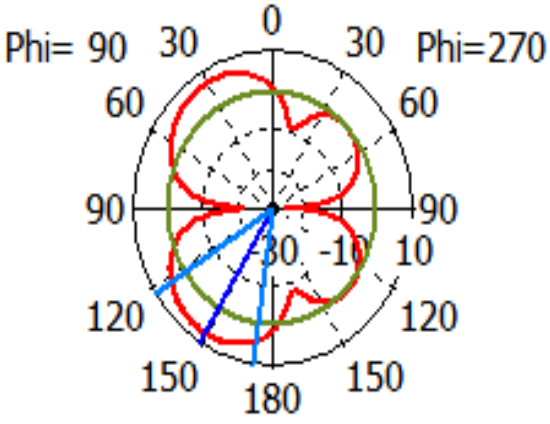

Figure 4.10 (d): Polar Radiation Pattern of Second Stage at 1.87 GHz

As depicted in figure 4.11, the third stage is designed by CST and as show in figure 4.12 (a) it gave return loss of -36.293 dB, and bandwidth efficiency 23 % at first resonant frequency 1.08 GHz. At the second resonant frequency 1.82 GHz, the return loss and bandwidth efficiency are -17.8 dB and 3 % respectively. Whereas in figure 4.12 (b) the efficiency bandwidths in the paper were 47.4 % at 0.98 GHz and 13.5 % at 1.84 GHz.

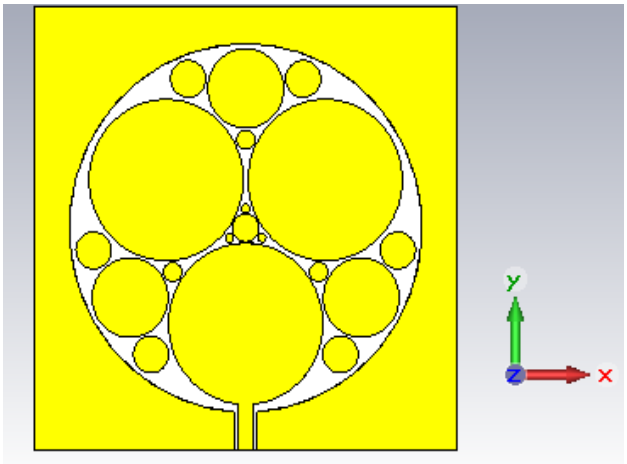

Figure 4.11: Design of Third Stage

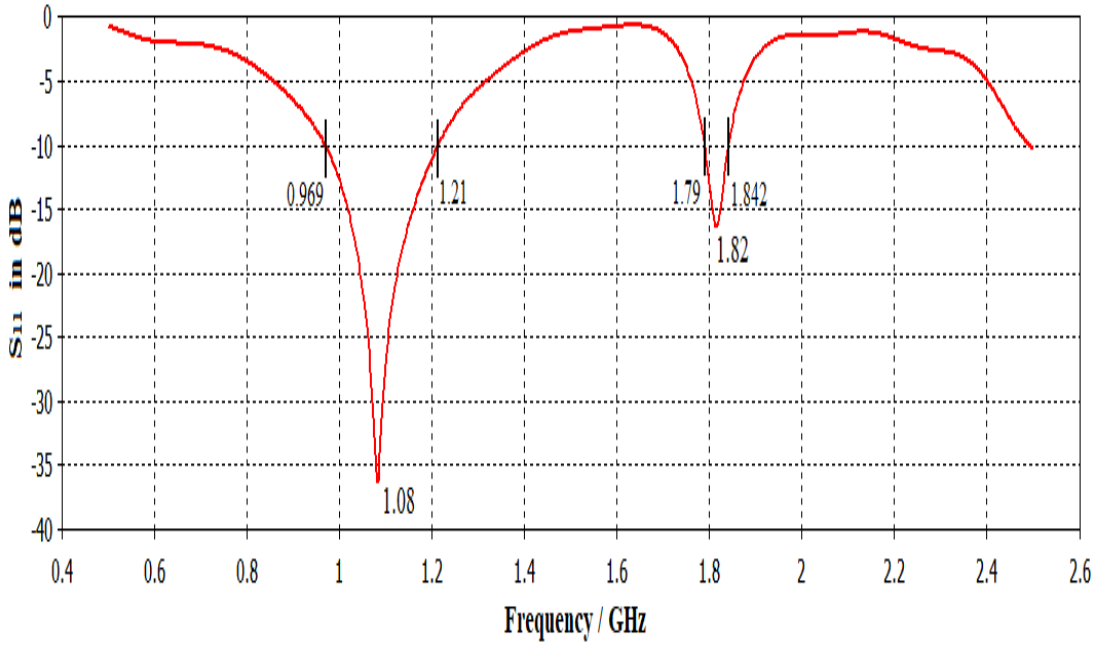

Figure 4.12 (a): Return Loss of Third Stage

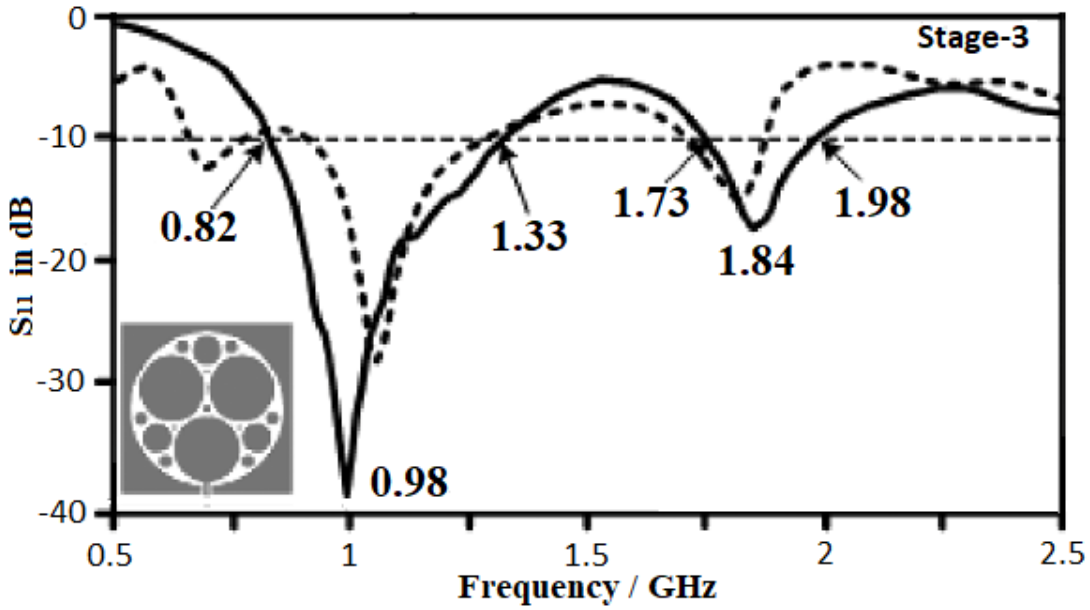

Figure 4.12 (b): Return Loss of [19]

It is worthy of note that the curve dotted is the simulation and the other curve is measurement.

Figure 4.13 (a, b) illustrates the radiation pattern in 3D and polar image respectively at 1.08 GHz. From this, the directivity and gain are denoted as 3.95 dB and 4.26 dB respectively, as compared with result of paper see figure 4.14.

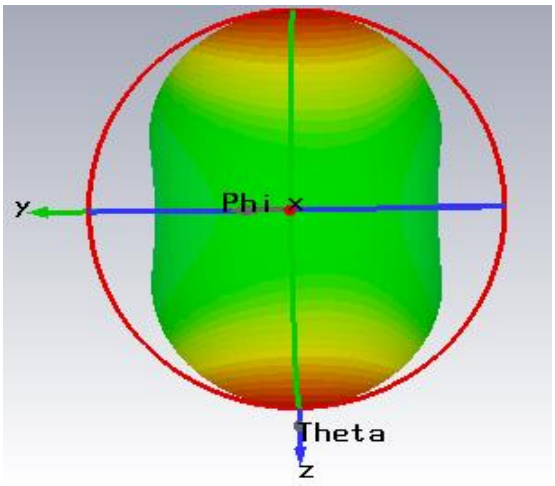

Figure 4.13 (a): 3D Radiation Pattern of Third Stage at 1.08 GHz

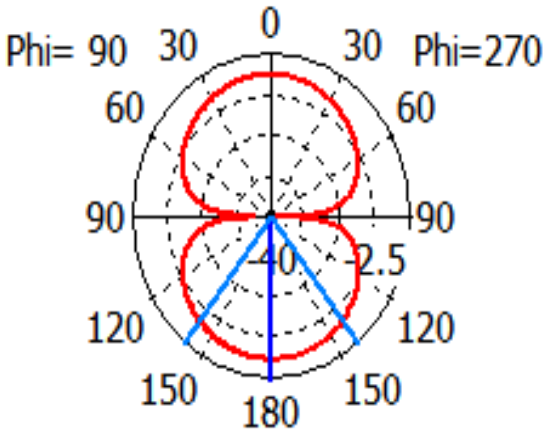

Figure 4.13 (b): Polar Radiation Pattern of Third Stage at 1.08 GHz

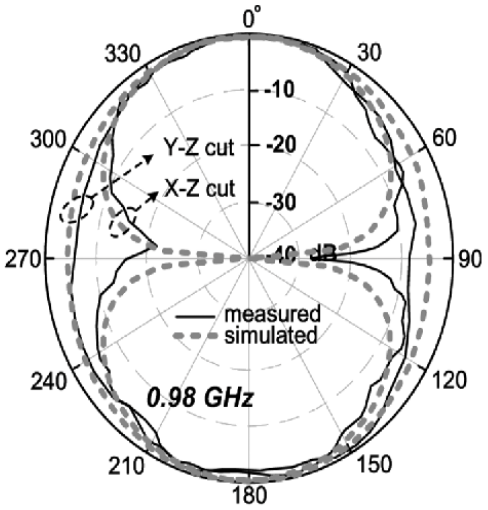

Figure 4.14: Radiation Pattern of Paper at 0.98 GHz [19]

Figure 4.15 (a, b) illustrates the 3D and polar radiation pattern. The directivity and gain are 6.72 dB and 6.47 dB at 1.82 GHz. The radiation pattern of reference paper is shown in figure 4.16 below.

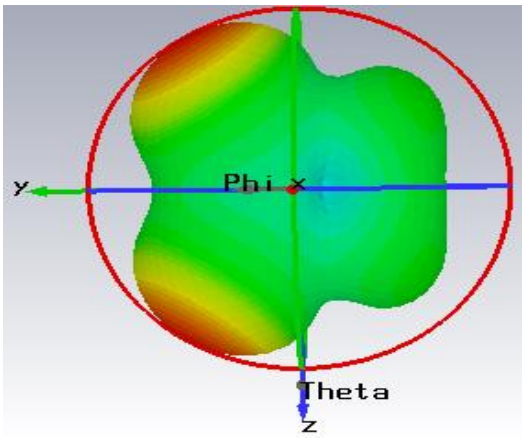

Figure 4.15 (a): 3D Radiation Pattern of Third Stage at 1.82 GHz

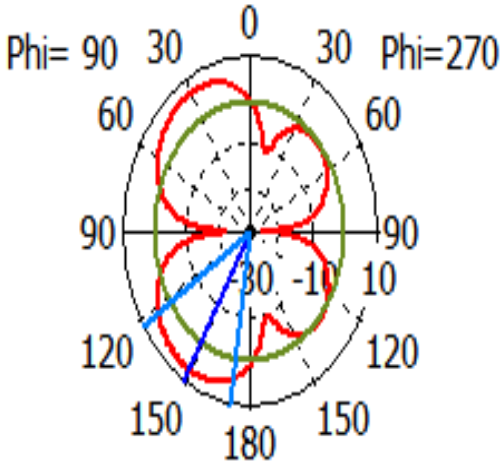

Figure 4.15 (b): Polar Radiation Pattern of Third Stage at 1.82 GHz

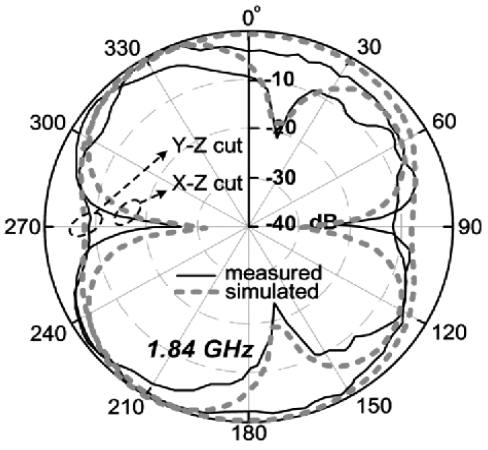

Figure 4.16: Radiation Pattern of Paper at 1.84 GHz [19]

When these results are compared with each other as contained in table 4.2, the directivity and gain at second stage are bigger than the others at first stage. It is clear that, the wideband is 32.2 % at frequency 1.16 GHz in second stage. Also, if the number of circles increases, the gain decreases. This is one of the disadvantages of fractal antenna earlier mentioned in the literature of this study [14].

Table 4.2: Discusses the Different between the Results of my Study.

Parameters	***Original***	***Stage 1***		***Stage 2***		***stage 3***	
Resonance frequency GHz	2.2249	1.67	1.926	1.16	1.87	1.08	1.82
Return loss dB	-38.762	-32	-37.86	-48	-21	-36.29	-16.5
Gain dB	6.75	3.97	4.83	4.41	6.55	4.26	6.47
Directivity dB	6.54	3.85	4.8	4.14	6.65	3.97	6.72
Bandwidth %	26.9	31.7	31.7	32.2	4	23	3

Table 4.3: Discusses the Different between the Results of [19].

Parameters	***Original***	***Stage 1***		***Stage 2***		***Stage 3***	
Resonant frequency GHz	2.22	1.63	1.92	1.13	1.87	0.98	1.84
Return loss dB	-35	-30.5	-35	-39	-21.5	-40	-19.8
Gain dB	-	-	-		-	-	-
Directivity dB	-	-	-	-	-	3.58	7.28
Bandwidth %	-	-	-	-	-	47.4	13.5

On the other hand, when the number of iteration increases, the multiband can be gotten. This is one of the numerous ways through which the fractal antenna is said to prove highly advantageous.

Based on this result, there was need to increase the number of circles with same radius 2.5 mm, and the multiband was derived at different resonant frequencies when six circles were added to the last design. As it clearly seen in figure 4.17. The number of circles in the last stage are 25.

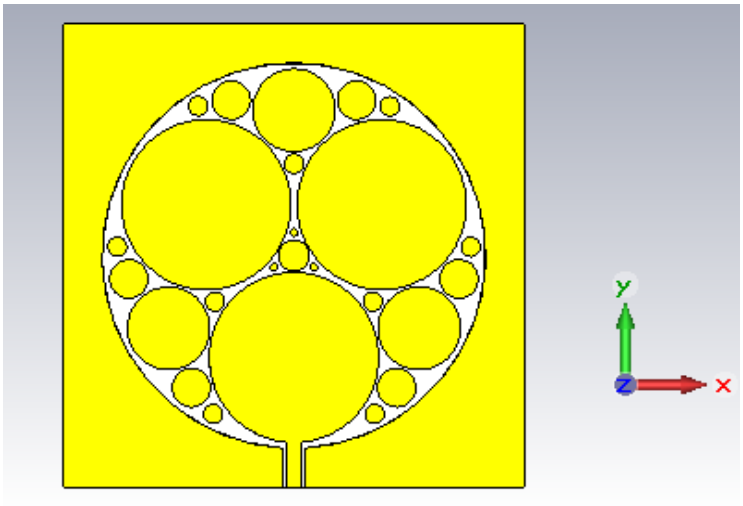

Figure 4.17: New Design

Table 4.3 illustrates the result of new design, and figure 4.18 shows the return loss. Here, there are four resonant frequencies three of them are lowered by 53.2 %, 35.4 % and 21.6 % at 1.04 GHz, 1.435 GHz and 1.74 GHz respectively. On the other hand, the last frequency 2.31 GHz is the upper frequency in the operation.

Table 4.4: Results of New Design

Centre Frequency (GHz)	**S11 (dB)**	**Upper Frequency (GHz)**	**Lower Frequency (GHz)**	**Bandwidth Efficiency (%)**	**Gain (dB)**	**Directivity (dB)**
1.04	-19.33	1.1447	0.89002	24.5	3.98	3.98
1.435	-15.1	1.4897	1.392	6.8	4.02	4.07
1.74	-11.6	1.7712	1.7149	3.2	5.75	6.27
2.31	-14.5	2.3881	2.2286	6.9	3.99	4.54

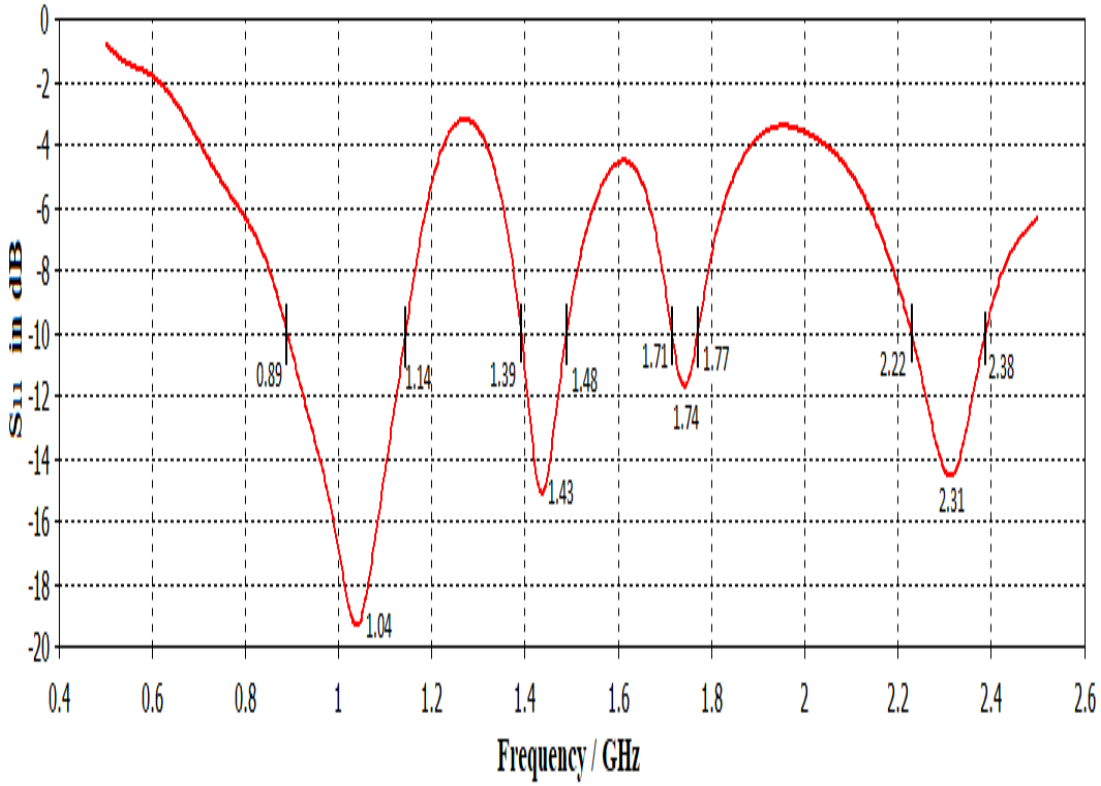

Figure 4.18: Return Loss of New Design

Figure 4.19 (a, b, c, d) illustrates the radiation pattern in polar image of the new design that measured at four resonant frequencies.

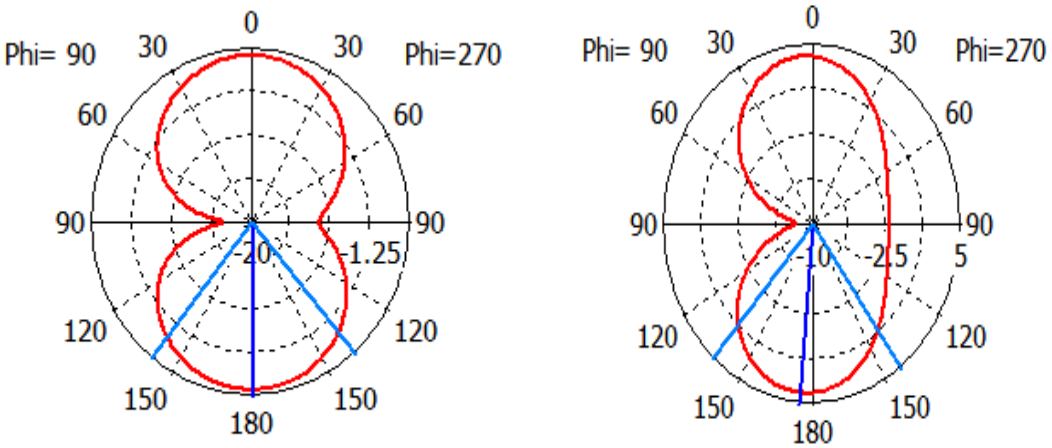

(a) $f_1 = 1.04$ GHz (b) $f_2 = 1.435$ GHz

Figure 4.19 (a, b): Polar Radiation Pattern of New Design at f_1 and f_2

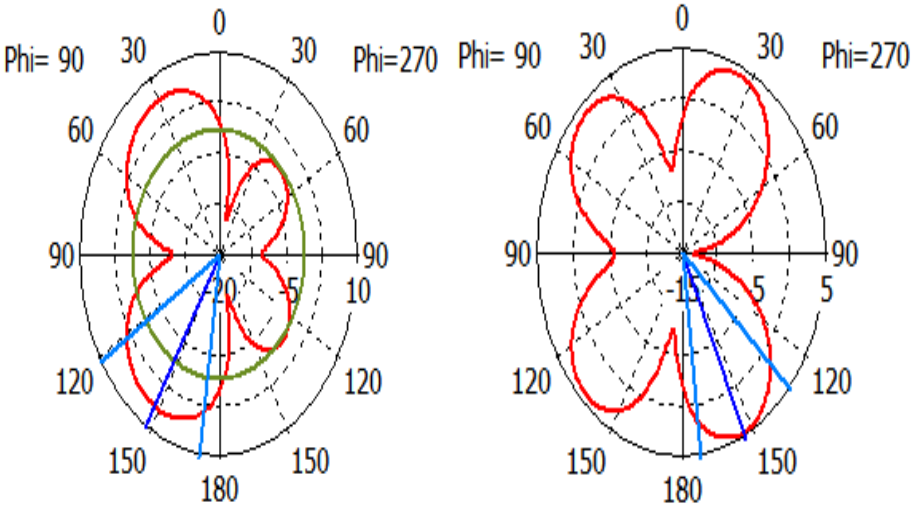

(c) f_3 = 1.74 GHz (d) f_4 = 2.31 GHz

Figure 4.19 (c, d): Polar Radiation Pattern of New Design at f_3 and f_4

The 3D patterns of the new design, measured for four frequencies of resonance are illustrated in figures 4.20 (a, b, c, d).

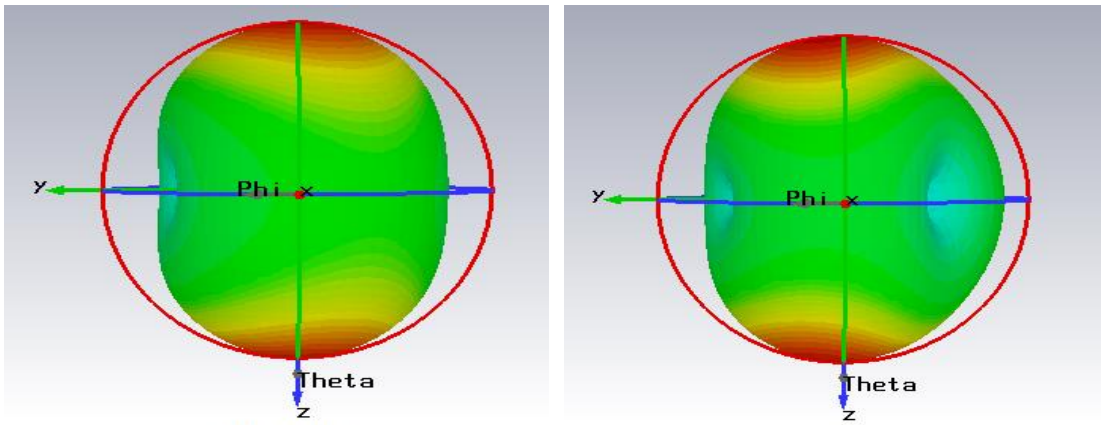

(a) f_1 = 1.04 GHz (b) f_2 = 1.435 GHz

Figure 4.20 (a, b): 3D Radiation Pattern of the New Design at f_1 and f_2

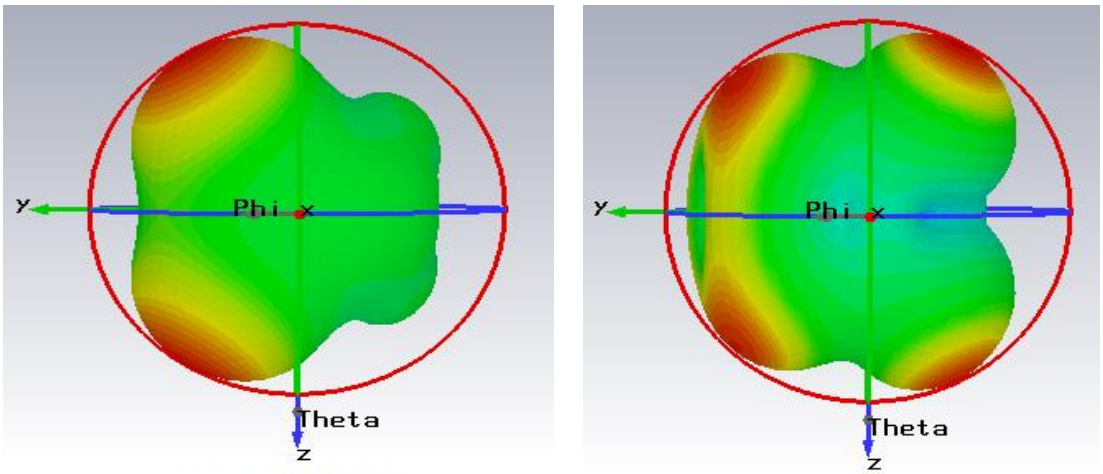

(c) $f_3 = 1.74$ GHz (d) $f_4 = 2.31$ GHz

Figure 4.20 (c, d): 3D Radiation Pattern of New Design at f_3 and f_4

As we can see from the range of frequencies covered by the proposed antenna, this antenna can be used in different applications that are in several areas such as GSM, WLAN, WIMAX, Microwave landing systems, Radio determination applications, Radar and Defence systems, etc.

Chapter 5

CUT IN GROUND DESIGN AND RESULTS

5.1 Introduction

In the engineering profession, professionals strive for best results. So in the course of this study efforts were made to change some of diminutions of old antenna design (like permittivity and thickness of substrate) to derive the best results possible in one of parameters such as return loss, bandwidth efficiency, gain and directivity. In this chapter, cutting in ground plane was done to get wider bandwidth [20]. H-shape and U-shape cuts were done in the ground plane of the fractal antenna at last stage. The results are compared with the previous results.

5.2 H-shaped Cut

It is widely known that the H-shaped cut is a popular solution used to have small size with high gain and wideband. This cut was used with circular fractal, and the results obtained were good, when the width of the cut is 8mm as we can see in figure 5.1.

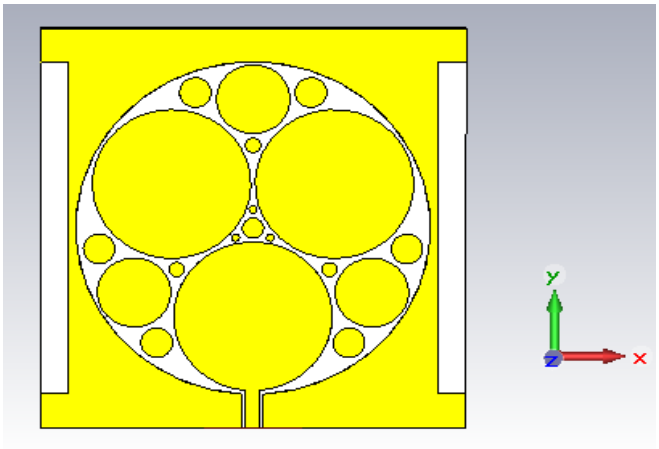

Figure 5.1: H-Shaped Cut in Ground Plane.

Figure 5.2 shows that the return loss of H-shaped was -33.556 dB and efficiency bandwidth 55.9 % at first frequency 0.958 GHz, and it was -15.304 dB and efficiency bandwidth 4.115 % at second frequency 1.74 GHz.

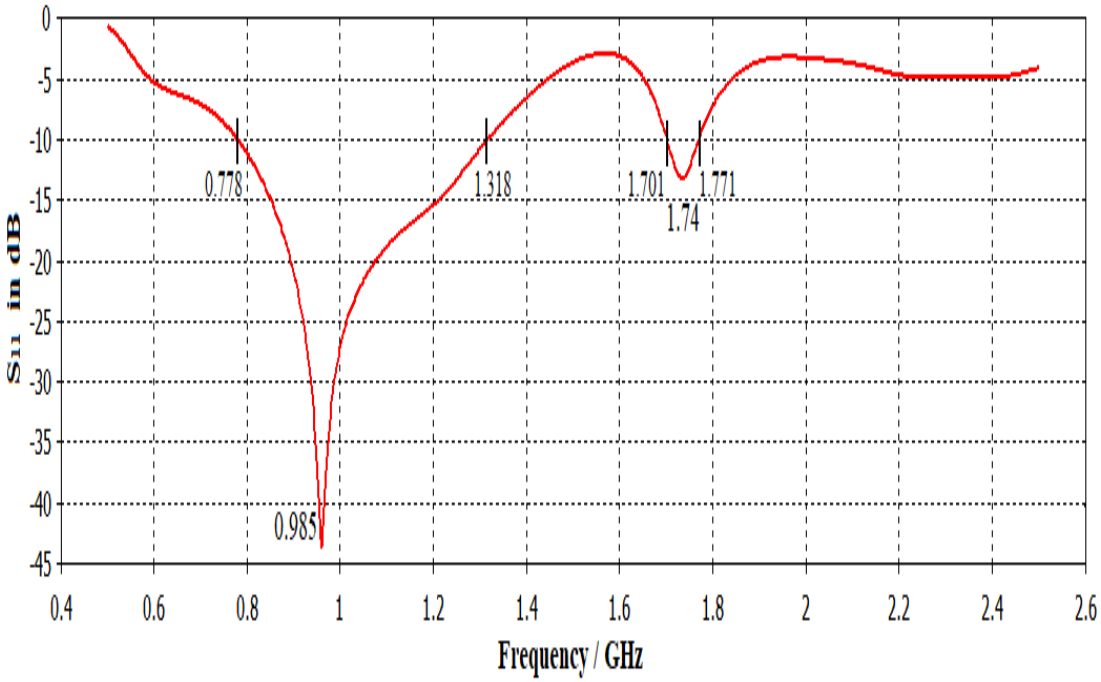

Figure 5.2: Return Loss of H-Shaped Cut

As we can see in figure 5.3 (a, b) the gain and directivity at 0.958 GHz are 3.43 dB and 3.13 dB respectively, and 6.52 dB, 6.61 dB at 1.74 GHz.

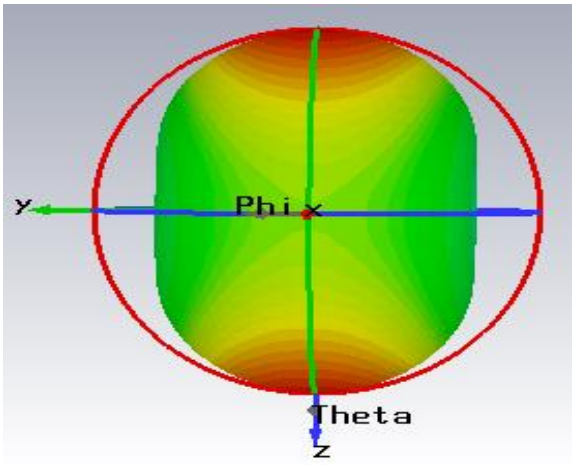

Figure 5.3 (a): 3D Radiation of H-Shaped Cut at 0.958 GHz

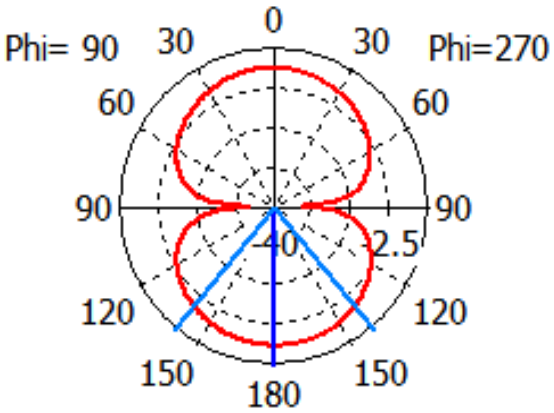

Figure 5.3 (b): Polar Radiation of H-Shaped at 0.958 GHz

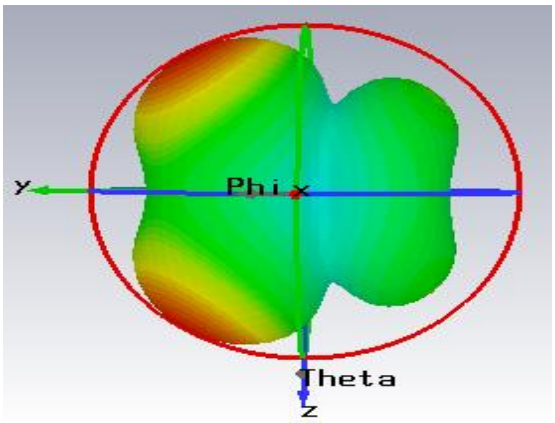

Figure 5.3 (c): 3D Radiation Pattern of H-Shaped Cut at 1.73 GHz

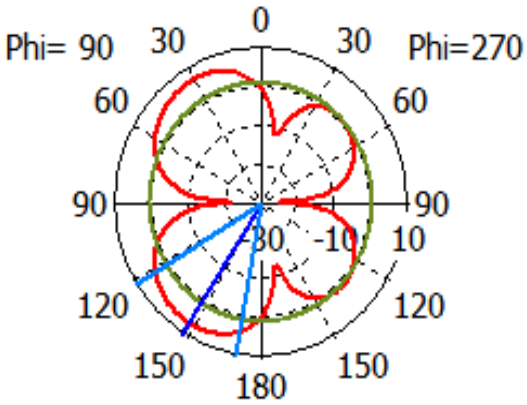

Figure 5.3 (d): Polar Radiation Pattern of H-Shaped Cut at 1.73 GHz

5.3 U-shaped Cut

In figure 5.4, the U-shaped cut of circular fractal antenna with same width of cut H-shaped is illustrated.

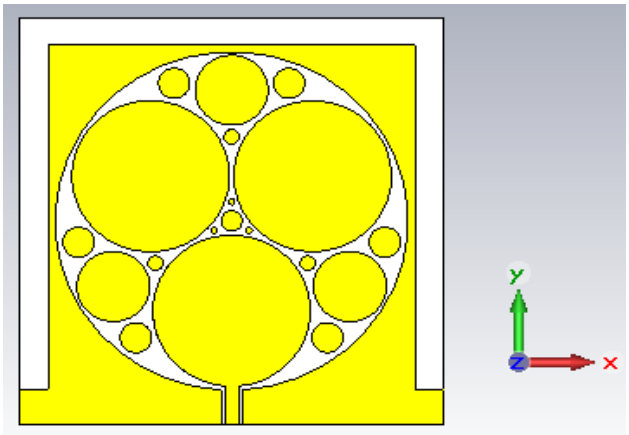

Figure 5.4: U-Shaped Cut in Ground Plane

Figure 5.5 shows that the return loss and the bandwidth efficiency at first frequency 1.004 GHz and second frequency 1.735 GHz were -25.184 dB, 45 % and -13.874 dB, 3.67 % respectively.

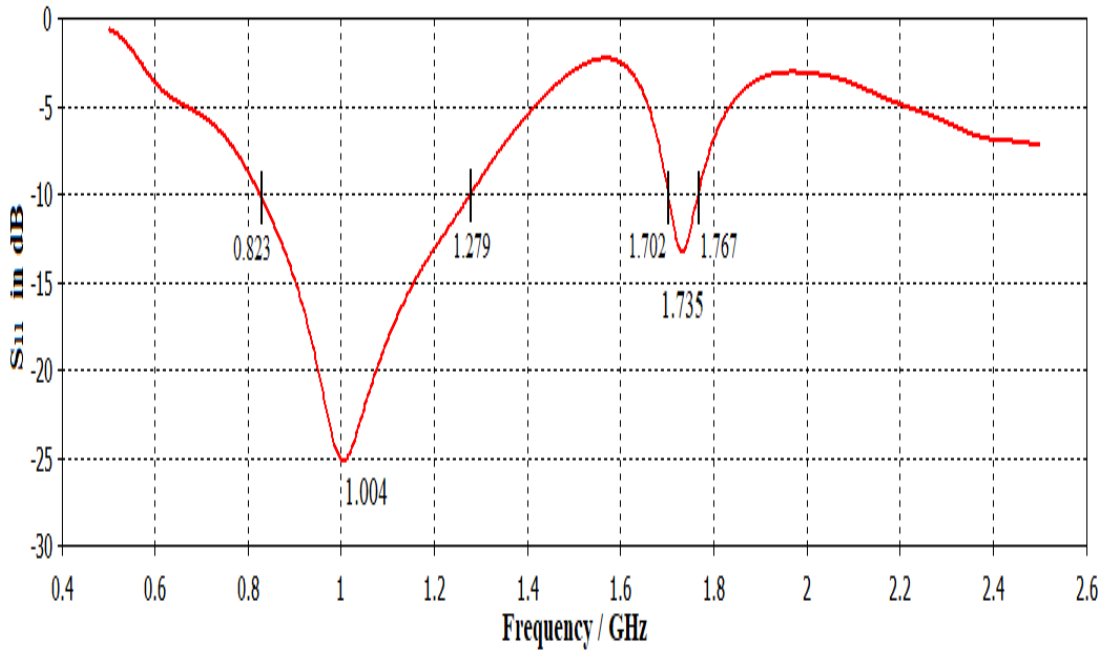

Figure 5.5: Return Loss of U-Shaped Cut

Figures 5.6 (a, b, c and d) show the 3D and polar radiation pattern of first and second resonant frequencies. The directivity and gain at these frequencies were 3.23 dB, 3.51 dB at 1.004 GHz, and 6.2 dB, 6.09 dB at 1.735 GHz respectively.

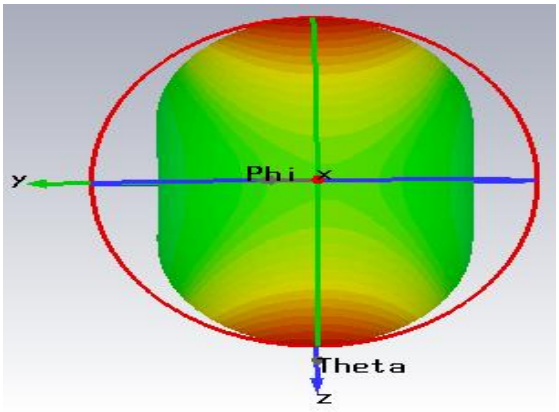

Figure 5.6 (a): 3D Radiation Pattern of U-Shaped Cut at 1.004 GHz

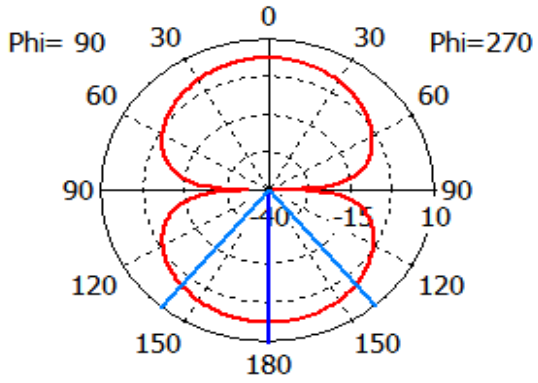

Figure 5.6 (b): Polar Radiation Pattern of U-Shaped Cut at 1.004 GHz

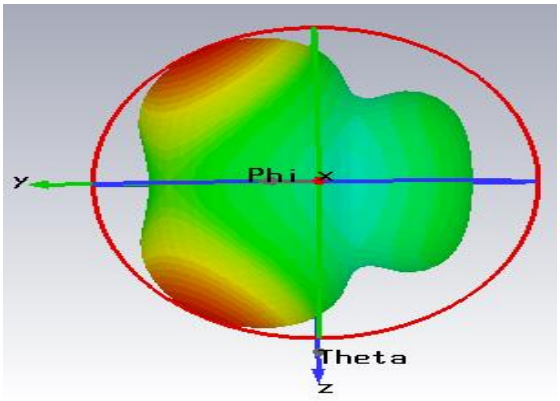

Figure 5.6 (c): 3D Radiation Pattern of U-Shaped Cut at 1.735 GHZ

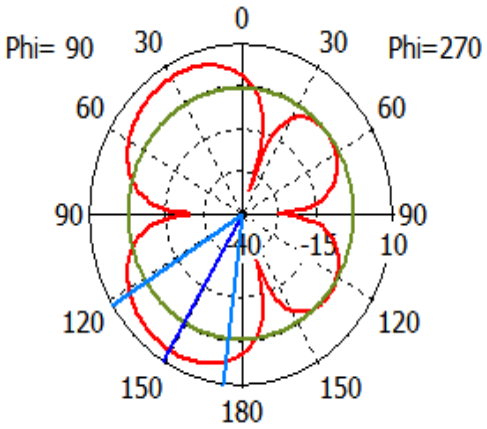

Figure 5.6 (d): Polar Radiation Pattern of U-Shaped Cut at 1.735 GHz

5.4 Comparing and Discussing the Results

Table 5.1: Discusses the Different between the Results of Every Design.

Parameters	***Third Stage***		***Cut H-shaped***		***Cut U-shaped***	
Frequencies GHz	1.08	1.82	0.958	1.74	1.004	1.735
Return loss dB	-36.29	-16.5	-33.556	-15.304	-25.184	-13.874
Directivity dB	3.97	6.72	3.13	6.61	3.23	6.2
Gain Db	4.26	6.47	3.43	6.52	3.51	6.09
Bandwidth %	23	3	55.9	4.115	45	3.67

From all indications, all designs gave dual-band and wideband, but when cut was used as another solution to have wideband, it provided a good solution. This is because the bandwidth efficiency improved at first frequency from 23 % at third Stage to 45 % at U-shaped then to 55.9 % at H-shaped. However, in both cases, the differences between gain and directivity is not high.

In figure 5.7 the return loss for every design are shown. Here, the resonance frequency 1.08 GHz of third Stage is lowered by 51.3 %, and the resonant frequency 0.958 GHz is lowered by 56.8 % at H-shaped. Whereas the resonant frequency 1.004 GHz is lowered by 54.8 % at U-shaped when compared to figure 4.2.

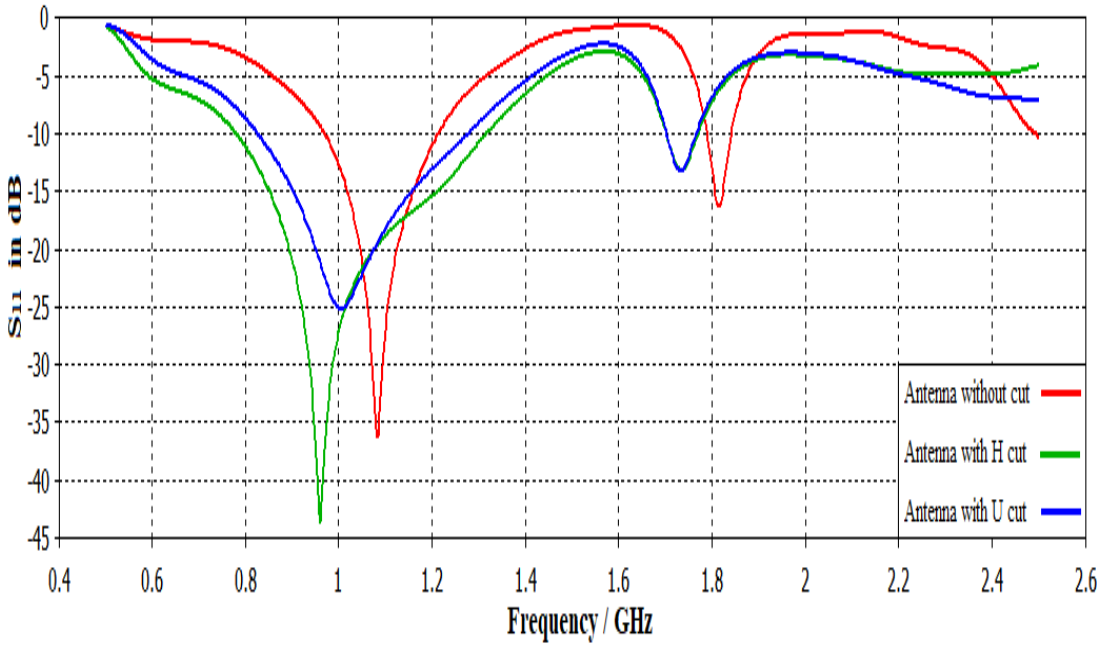

Figure 5.7: Return Loss of Three Designs

Chapter 6

CONCLUSION AND FUTURE WORK

6.1 Conclusion

This study is about the use of fractal geometries for obtaining dual-band and wideband. For this purpose, the Descartes Circle Theorem was applied with circular fractal antenna design in coplanar waveguide fed for four iterations. Two wideband responses were obtained, 23 % at resonance 1.08 GHz, and 3 % at 1.82 GHz. The resonant frequency was lowered by 51.3 %. The directivity was 6.54 dB when the original design was deployed and it was 3.97 dB and 6.72 dB for the resonant frequencies 1.08 GHz and 1.82 GHz respectively. It is clear from the above findings that using fractal antenna geometries, help to have wideband with good gain and directivity. Also when the number of iterations is increased, multiband can be obtained, which can be utilised in different communication applications.

A new approach using U-shaped and H-shaped with circular fractal of third iteration gave good results, enhancing the bandwidth efficiency from 23 % to 45 % and 55.9 % for U-and H-shaped designs respectively.

In the end, the objective the researcher initiated and embarked on this study, that is, to design a fractal antenna with dual-band and wideband, was successful.

6.2 Future Work

Despite the numerous research endeavours by different scholars in the electrical engineering profession, the area of fractional antenna is still in its infancy and as such there is still limited literature. Based on the findings of this study, it is clear that there are research prospects in the area of configuration. On this note, the researcher suggests that future research work should be considered on the integration of reusable technology to make the antenna suitable for switching to the required operating rang.

REFERENCES

[1] J. W. Greiser, “Coplanar strip line antenna”, *Microw. J,* vol. 19, no. 10, pp.47–49, 1976.

[2] T. A. Denidni and M. A. Habib, “Broadband printed CPW-fed circular slot antenna”, *Electron. Lett.,* vol. 42, no. 3, pp. 135–136, 2006,

[3] S. N. Sinha and M. Jain, “A self-affine fractal multiband antenna,” *IEEE Antennas Wireless Propag. Lett,* vol. 6, pp. 110–112, 2007.

[4] J. C. Liu, Y. J. Liu, D. C. Chang, C. C. Chang, and C. Cheng, “Fractal multi- band antennas based on Lotus-pod patterns,” *Microw. Opt. Technol. Lett,* vol. 33, no. 3, pp. 223–228, May. 2002.

[5] J. C. Liu, D. C. Chang, D. Soong, C. H. Chen, C. Y. Wu, and L. Yao, “Circular fractal antenna approaches with Descartes circle theorem for multi-band/wide-band applications” *Microw. Opt. Technol. Lett,* vol. 44, no. 5, pp. 404–408, Mar. 2005.

[6] C. A. Balanis, “Antenna theory analysis and design”, A *Fundamental Parameters of Antennas &Microstrip Antennas*, pp. 27-104 & pp 811-872, 2005, Published by John Wiley & Sons, Inc., Hoboken, New Jersey.

[7] S. Vajha and S.N Prasad, “Design and modelling of a proximity coupled patch antenna”, *Antennas and Propagation for Wireless Communications, IEEE. APS Conference,* pp. 43-46, 6-8 Nov. 2000.

[8] S. Bisht, S. Saini, Dr. V. Prakash and B. Nautiyal, " Study the various feeding techniques of microstrip antenna using design and simulation using CST microwave studio", *International Journal of Emerging Technology and Advanced Engineering*, vol. 4, Issue. 9, Sept. 2014.

[9] E. S. Angelopoulos, A. Z. Anastopoulos, D. I. Kaklamani, A. A. Alexandridis, F. Lazarakis, and K. Dangakis, “Circular and elliptical CPW-fed slot and microstrip -fed antennas for ultra wideband applications,” *IEEE Antennas Wireless Propag Lett.*, vol. 5, pp. 294–297, 2006.

[10] Y. Huang and K. Boyle, “Antennas from theory to practice”, *Coplanar Waveguide*, 2008, pp. 65-66, Published by John Wiley & Sons Ltd, The Atrium, Southern Gate, Chichester, West Sussex, PO19 8SQ, United Kingdom.

[11] D. H. Werner and S. Ganguly, “An overview of fractal antenna engineering research,” *IEEE Antennas Propag. Mag.*, vol. 45, no. 1, pp. 38–57, Feb. 2003.

[12] C. Puente, J. Romeu and A. Cardama, “The koch monopole: a small fractal antenna”, *IEEE Trans. On Antennas and Propagation,* vol.48, pp. 1173- 1781, 2001.

[13] “Sierpinski gasket fractal iteration”, available at http://math.bu.edu/DYSYS/chaos-game/sierp-det.GIF, last accessed June 2018.

[14] A. Tiwari, Dr. M. Rattan and I. Gupta, "Review on: fractal antenna geometries and its applications”, International *Journal of Engineering and Computer Science ISSN:2319-7242*, vol. 3, Issue. 9, pp. 8270-8275, Sept. 2014.

[15] J. C. Liu, D. C. Chang, D. Soong, C. H. Chen, C. Y. Wu, and L. Yao, “Circular fractal antenna approaches with Descartes circle theorem for multi-band/wide-band applications”, *Microw. Opt. Technol. Lett*, vol. 44, no. 5, pp. 404–408, Mar. 2005.

[16] J. L. Heureux, G. Scarr, Y. Shtiui and Y. Tian," Descartes and the apollonian gasket", *Math 445 A - Group Project*, June 5th. 2013.

[17] J. C. Lagarias, C. L. Mallows and A. R. Wilks," Beyond the descartes circle theorem", *AT&T Labs, Florham Park*, NJ 07932-0971, January 8. 2001.

[18] J. C. Liu, D. C. Lou, C. Y. Liu, C. Y, Wu, and T .W. Soong," Precise determinations of the CPW-fed circular fractal slot antenna", *Microwave and Optical Technology Letters*, vol.48, no. 8, August. 2006.

[19] Dau-Chyrh Chang, Bing-Hao Zeng and Ji-Chyun Liu, " CPW-fed circular fractal slot antenna design for dual-band applications", *IEEE Transactions on Antennas and Propagation*, vol. 56, no. 12, December. 2008.

[20] R. Kumar, J. P. Shinde and M. D. Uplane, "Effect of slots in ground plane and patch on microstrip antenna performance", *International Journal of Recent Trends in Engineering*, vol 2, no. 6, November. 2009.